

1962

A model study of the application of roof bolts under unsymmetrical loading conditions

Friedrich H. K. Esser

Follow this and additional works at: https://scholarsmine.mst.edu/masters_theses



Part of the [Mining Engineering Commons](#)

Department:

Recommended Citation

Esser, Friedrich H. K., "A model study of the application of roof bolts under unsymmetrical loading conditions" (1962). *Masters Theses*. 4166.

https://scholarsmine.mst.edu/masters_theses/4166

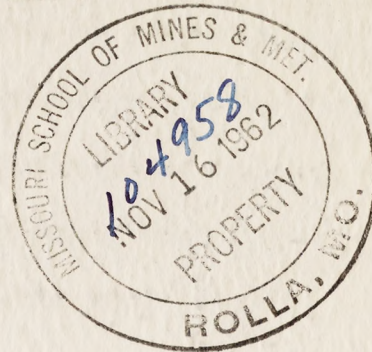
This Thesis - Open Access is brought to you for free and open access by Scholars' Mine. It has been accepted for inclusion in Masters Theses by an authorized administrator of Scholars' Mine. This work is protected by U. S. Copyright Law. Unauthorized use including reproduction for redistribution requires the permission of the copyright holder. For more information, please contact scholarsmine@mst.edu.

T 1419

H 6338

A MODEL STUDY OF THE APPLICATION
OF ROOF BOLTS
UNDER UNSYMMETRICAL LOADING CONDITIONS

BY
FRIEDRICH H. K. ESSER



A
THESIS

Submitted to the faculty of the
SCHOOL OF MINES AND METALLURGY OF THE UNIVERSITY OF MISSOURI
in partial fulfillment of the requirements for the
Degree of
MASTER OF SCIENCE IN MINING ENGINEERING

Rolla, Missouri

1962

Approved by

Rodney S. Carle (Advisor)

R. F. Davidson

Ray E. Morgan
George B. Clark

ABSTRACT

When coal is extracted by the long wall mining method, two gate-roads on either side of the working face are driven with the advancing operation. In the surroundings of these openings the state of stress which existed prior to mining is not only disturbed by the drifting process of the gate-roads but also by the coal extraction in the long wall, resulting in an "unsymmetrical" stress distribution. Varying incremental pressure components and the high complexity of strata movements make it extremely difficult to control the rock behavior under unsymmetrical conditions by conventional support. Application of roof bolts as an auxiliary support can improve the control of the strata surrounding long wall gate-roads.

To indicate the qualitative effect of roof bolts on the stress distribution around underground openings in stratified rock under unsymmetrical loading conditions, composite models made of photo-elastic material were tested in a 6 ft. diameter centrifuge, providing proper loading conditions. Stress distributions were permanently "frozen" into the models while under load.

Test results indicate that the high shearing stresses which occur near the rigid abutment of the long wall gate-road and the bending stresses in the roof beams can be reduced considerably by the application of roof bolts in proper pattern arrangements.

Since this study was concerned with the development of an experimental technique and simple structural conditions were chosen, an extension of this investigation to more complicated conditions is possible.

ACKNOWLEDGEMENT

The writer wishes to thank Mr. R. D. Caudle, Research Instructor in the Department of Mining Engineering, Missouri School of Mines and Metallurgy, for his aid and advice in performing the present research and his help in preparation of this thesis. He also is grateful to Professor Dr. G. B. Clark, Associate Director of the Research Center of this School, for his criticism of the manuscript. Appreciation is expressed to Mr. R. F. Bruzewsky, Associate Professor of Mining Engineering for his advice and assistance in the preparation of the photographs contained in this paper.

TABLE OF CONTENTS

	PAGE
ABSTRACT	i
ACKNOWLEDGEMENT	ii
TABLE OF CONTENTS	iii
LIST OF FIGURES AND DIAGRAMS	vi
LIST OF PHOTOGRAPHS	vii
NOTATION	x
CHAPTER	
I. INTRODUCTION	1
History of Roof Bolting	1
Purpose of Investigations	2
II. REVIEW OF LITERATURE	6
Stresses and Movements in the Strata around	
Openings	6
Symmetrical Case: Opening in the Room and	
Pillar Mining Method	7
Unsymmetrical Case: Opening in the Long Wall	
Mining Method	10
Additional Pressure	10
Relaxation Movement	18
Theory and Practice of Roof Bolting in Stratified	
Rock	20

	PAGE
Suspension Support	23
Beam Theory	25
Increase in Frictional Resistance to	
Bedding-plane Slip	30
Shear Strength of the Roof Bolts	31
Shear Reinforcement of the Rock	31
Tensile Reinforcement of the Rock	33
Model Study	36
Theory of Model Study	36
Photo-elasticity as Applied to Model Study . .	40
"Stress-Freezing" Technique in Model Study . .	47
Application of Model Study to Roof Bolting . .	50
III. MODEL STUDY OF THE APPLICATION OF ROOF BOLTS UNDER	
UNSYMMETRICAL LOADING CONDITIONS	59
Theoretical Background of the Experiments	60
Experimental Instrumentation	62
Centrifugal Testing Apparatus	62
Rotor	63
Model Holders and Counterweight	65
Housing Tank	68
Accessory Equipment	69
Photo-elastic Equipment	70
Model Design	71

	PAGE
Test Procedure	73
Casting and Curing Process	73
Preparing Model for Test	75
Loading Process	78
Preparing Model for Analysis	79
Analysis of the Models	80
IV. SUMMARY AND CONCLUSIONS	98
REFERENCES	R1
VITA	R6

LIST OF FIGURES AND DIAGRAMS

FIGURE	PAGE
1. Stress Distribution around Openings (after Dorstewitz)	8
2. Schematic View of a Long Wall Operation	12
3. Pressure "wave" accompanying an advancing Long Wall	14
4. "S" - Curve	16
5. "S" - Curve with Point of Inflection (after Dubois)	17
6. Two Roof Bolts as Suspension Support	24
7. "Plug-effect" of Roof Bolts	24
8. Stress Distribution along the Beam in the immediate Roof of an Mine Opening (after Panek)	28
9. Bore Hole Displacement	29
10. Increase of frictional Resistance to Bedding-plane Slip by Roof Bolts	32
11. Shear Reinforcement of the Strata by Roof Bolts	34
12. Tensile Reinforcement of the Strata by Roof Bolts	35
13. Fringe Order along horizontal Diameter Disk with time as Parameter	50a
14. Roof Bolt Pattern in Long Wall Gate-Roads (after Bals)	58
15. Photo-elastic Model representing a Section through a Long Wall Gate-Road	72
16. Standard Time Schedule for the Test Series including the "Stress-Freezing" Process	74

LIST OF PHOTOGRAPHS

PICTURE	PAGE
1. Influence of Strata Bedding and Friction between Bedding on the Stress Distribution around Rectangular Openings	9
2. Influence of Strata Bedding and Friction between Bedding on the Stress Distribution around Circular Openings (after Sonntag).	9
3. Stress Distribution in the Surroundings of a Long Wall Operation with thick Beds (after Sonntag) . .	13
4. Stress Distribution in the Surroundings of a Long Wall Operation with low Friction between the Beds (after Sonntag)	13
5. Stress Distribution in the Surroundings of a Long Wall Operation with thinner Beds (after Sonntag). .	13a
6. Pseudo-plastic Behavior of the Strata in a Long Wall Gate-Road	22
7. "Quarter-Moon" Shape in a Borehole caused by Bed Displacement	22
8. Polariscopes	46
9. Three-dimensional Model representing a Section through a Long Wall Gate-Road (after Bals)	57

PICTURE	PAGE
10. Centrifugal Testing Apparatus	64
11. Model Holder I and II	66
12. Model Holder II	66
13. Counterweight	67
14. Balance	67
15. Mold for the Casting Process	77
16. Roof Bolts, Washers and Nuts as used in the Model Study	77
17. Unsymmetrical Model after Shaping and Polishing . . .	81
18. Symmetrical Model after Shaping and Polishing with Roof Bolts	81
19. Test (6): Fringe Pattern of a Symmetrical Model . .	84
20. Test (7): Fringe Pattern of an Unsymmetrical Model .	84
21. Test (13): Fringe Pattern of an Unsymmetrical Model.	87
22. Test (8): Fringe Pattern of an Unsymmetrical Model with three Vertical Roof Bolts	87
23. Test (14): Fringe Pattern of an Unsymmetrical Model with three Holes (45° , 60° and 90°)	90
24. Test (15): Fringe Pattern of an Unsymmetrical Model with three Roof Bolts (90° , 60° and 45°)	90
25. Test (16): Fringe Pattern of an Unsymmetrical Model with one Roof Bolt (45°)	92

PICTURE	PAGE
26. Test (17): Fringe Pattern of an Unsymmetrical Model with two Roof Bolts (45° and 45°)	92
27. Test (18): Fringe Pattern of an Unsymmetrical Model with one Roof Bolt (60°).	93
28. Test (19): Fringe Pattern of an Unsymmetrical Model with three vertical Roof Bolts	93
29. Test (20): Fringe Pattern of an Unsymmetrical Model with three Roof Bolts (45° , 60° and 60°)	95
30. Test (10): Unsymmetrical Model with three Holes (45° , 90° and 45°). The lower Beam failed in Tension near both Abutments	95

NOTATION

σ	=	Stress (psi)
ϵ	=	Strain
$\sigma_{1/2}$	=	Principal Stresses (psi)
τ	=	Shearing Stress (psi)
x, y, z	=	Cartesian Coordinates
w	=	Unit Weight (lb./cu.in.)
w^b	=	Unit Weight of Bolt Material (lb./cu.in.)
E	=	Modulus of Elasticity (psi)
E^b	=	Modulus of Elasticity of Bolt Material (psi)
ν	=	Poisson's Ratio of Roof Rock
ν^b	=	Poisson's Ratio of Bolt Material
σ_{sf}	=	Outer Fiber Bending Stress when both Friction and Suspension Effects are present (psi)
σ_n	=	Outer Fiber Bending Stress when neither Friction nor Suspension Effects are present (psi)
L	=	Roof Span (inches)
t	=	Thickness of the Bolted Roof Beds (inches)
δ	=	Roof Deflection (inches)
D_f	=	Fractional Change in the Outer-fiber Bending Stress due to the Friction Effect
D_s	=	Fractional Change in the Outer-fiber Bending Stress due to the Suspension Effect
$1 + u_1$	=	Relative Flexural Rigidity
μ	=	Friction Value
F	=	Coefficient of Friction on Bedding Plane
b	=	Spacing between the Bolt Sets along the Opening (inches)
h	=	Bolt Length (inches)
d	=	Bolt-hole Diameter (inches)
d^b	=	Bolt Diameter (inches)
P	=	Bolt Tension (lbs.)
K	=	Bolts per Set across the Opening
M	=	Moment applied to Beam at the Support (lb.in.)
A	=	Centrifugal Loading Ratio ("g's")
g	=	Acceleration of Gravity (32.2 ft./sec. ²)
m	=	Mass Unit
R	=	Radius of Rotation of the Centrifuge
N	=	Number of Revolutions (R.P.M.)
ω	=	Angular Velocity (/sec)
s	=	Scale Factor

- β, γ, ϵ = Factors varying with the Location and Number of the Attachments (Bolts)
- v = Velocity of Light in the Medium Surrounding the Photo-elastic Model
- v_1, v_2 = Velocity of Light along the Principal Planes in the Photo-elastic Model
- C = Constant
- α = Angle between the Plane of Vibration of the Plane polarized Light and the σ_1 Direction
- Ω = Angular Frequency of the incident Light
- n = Fringe Order
- f = Material Fringe Value (psi-in./fringe)
- T = Thickness of the Model (inches)

CHAPTER I

INTRODUCTION

History of Roof Bolting

Roof bolting as a new kind of support was introduced in the mining industry in the last century. The application was, however, very sporadic and mostly restricted to experimental work. In 1880, MUELLER⁽¹⁾ mentioned roof bolts for the first time as used in a tunnel operation in the Swiss Alps. As reported by BUSCH⁽²⁾, a few attempts have been made since 1912 in Upper Silesia in Germany to reinforce roadway walls, by this method, in coal mines. In 1917, BALWIN⁽³⁾ introduced this new support in the American coal mining industry (Sagamore Mine of the Pocahontas Fuel Company). The beginning, however, of broad application and scientific study was made after 1945, when the mining industry in the United States installed many roof bolts under various conditions. In the past seventeen years a remarkable, continuous increase was achieved and most countries with underground operations followed the example given by the United States. In table (1) the total number of roof bolts installed in some important mining countries is listed for the year 1958.

TABLE I⁽⁴⁾

Country	Number of bolts
USA	50,000,000
Great Britain	250,000
West Germany	180,000 (without Saarld.)
France	112,000
Saarland	33,600
Poland	12,000
Netherland	3,500
Austria	1,600
USSR	Experimental status
Bulgaria	"
Belgium	"
Japan	"

Purpose of Investigation

Numerous publications have been presented in this new field of support since 1945 in the United States, Austria, Bulgaria, Canada, France, Germany, Great Britain, Netherland, Poland, Russia and

Sweden. In addition to these sources the author obtained information from many manufacturers of roof bolt equipment and accessories, and evaluated the results of private correspondence with mining organizations, research institutes and universities in the United States and Europe.

The wide application of the long wall mining method in Europe, Japan and elsewhere results in an unsymmetrical loading distribution around the gate-roads driven along each side of the extracted area. Considerable convergence occurs on the side of the coal extraction which cannot be avoided even by stowing, cribs or chocks. The high costs of conventional support* as used in long wall gate-roads, which have to be repaired several times and to be renewed in some cases, justify further investigations of the application of roof bolts as an auxiliary support.

The complicated stress conditions around long wall gate-roads make a theoretical approach difficult and restrict study to experimental investigations. Although many series of measurements of pressure and convergence, performed in coal mines all over the world, have improved the knowledge of roof bolt support in these workings, sufficient data have not been obtained to provide a complete solution of this problem.

*All kinds of support are defined as conventional which reinforce the strata from within the opening while roof bolts act in the strata itself.

Based on the literature study concerned with this subject the author decided to approach the problem by means of model experiments. Some previous attempts have been made to find the effect of roof bolts by duplicating the conditions existing underground in models. The investigators assumed that the stress distribution around the mine openings was symmetrical, as occurs in the roadways of the most American coal mines using the room and pillar mining method; that is, coal is left on both sides in the abutments.

In the present investigation unsymmetrical stress conditions were duplicated with three-dimensional models representing a section through a gate-road; the subsiding area was simulated with sheets of foam rubber. In order to maintain the stress magnitude and distribution, and the distortion and convergence of the strata, at scale proportions, where roof bolts are installed, variable body forces and proper loading conditions on the model were obtained by means of a 6 ft. diameter centrifuge. A technique for the usage of bi-refrangent plastic material in the centrifuge was developed to indicate the stress distribution by means of photoelastic effects. Fringes showing lines of equal maximum shearing stress were "frozen" in the model under load in the centrifuge and later analyzed with the aid of a polariscope. Different cases, with and without bolts, were compared and various pattern arrangements were designed.

Since rock does not behave strictly as an elastic body when under stress, the analysis of the results in this photo-elastic investigation must be qualitative rather than quantitative, and the results are obviously limited in application. Possible studies with a brittle material and more complicated conditions, such as inclined formations, varying thicknesses of beds and different moduli of elasticity, open a wide field for a continuation of this basic roof bolt study concerned with unsymmetrical loading conditions.

CHAPTER II

REVIEW OF LITERATURE

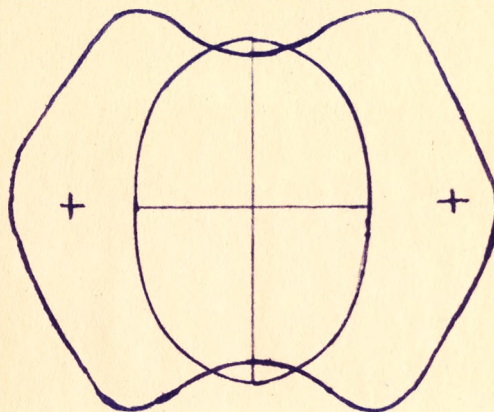
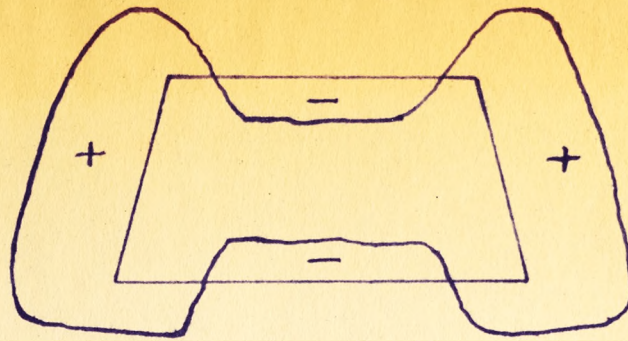
Stresses and Movements in the Strata Around Openings

For any problem dealing with roof bolting, a sufficient knowledge of the stresses and the movements in the strata around openings is necessary. The results of studies made by many authors^(4 to 20) lead to the following conclusions: When an excavation is mined in rock at depth, the stress distribution is readjusted in such a way, that a concentration of stress occurs in the immediate vicinity of the opening. The magnitude of the maximum stress which occurs is a function of (1) the geometry of the opening, (2) the physical properties of the material and (3) the state of the stress which existed prior to mining; and diminishes rapidly with increasing distance from the opening. A condition can exist, therefore, in which local stress at one or more points in the material surrounding the excavation exceeds the strength of the rock. The failure which originates at one of these points will propagate into the surrounding material and a zone of fractured rock will be formed around the opening. This fracture zone will become stable when the strength of the rock is no longer exceeded by the stress at any point in the material surrounding the excavation.

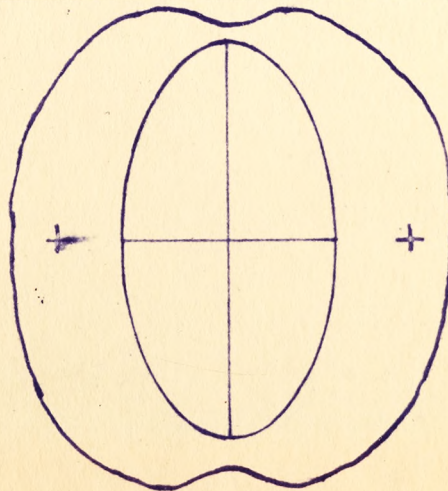
The influence of the geometry of the opening, the properties of the rock and the original stress field upon symmetrically loaded openings was in general investigated and described by PANEK⁽⁵⁾, OBERT, DUVALL and MERILL⁽⁶⁾ et al. Almost the same results were obtained in an independent study by DORSTEWITZ⁽⁷⁾ in 1941 who summarized in three significant pictures, as shown in Figure 1, a study of stress distribution around openings. An elliptical shape shows the lowest stress concentration, wherein the best height/width ratio is dependent on the stress field.

Symmetrical Case : Openings in the Room and Pillar Mining Method

SONNTAG⁽⁸⁾ performed the first photo-elastic study of stratified rock, which occurs in coal depositions. He found a remarkable influence of the bed thickness and the friction between the beds on the degree of stress concentration. This is shown in the Pictures 1 and 2, where rectangular and circular openings are loaded with vertical pressure. The tensile stress in the back is 1.7 and 1.5 times, respectively, the overlying pressure P and indicates the critical failure points, since the tensile strength of rock is known to be $1/8 - 1/40$ of its compressive strength. The results of these studies are applicable to roadways as utilized in the room and pillar mining



Height/Width
3 / 2

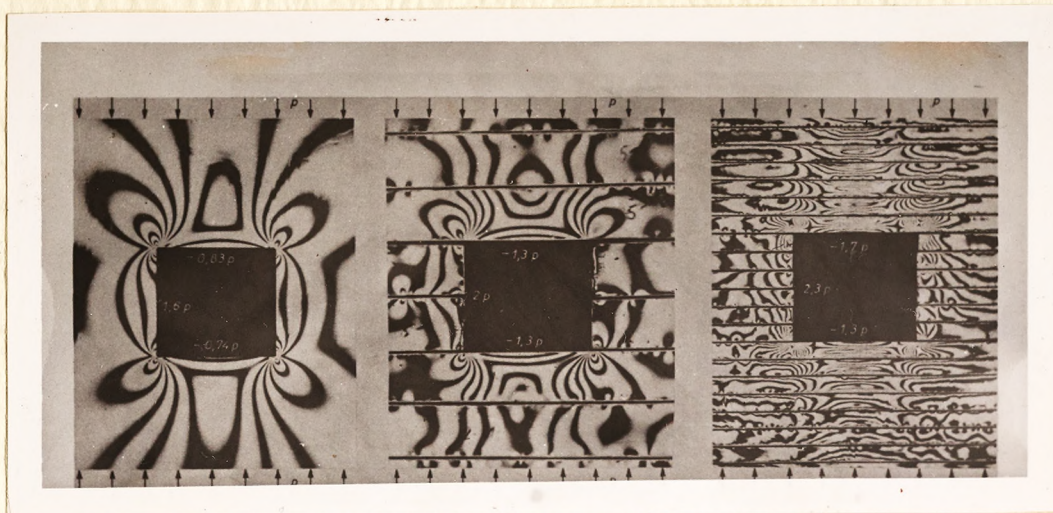


Height/Width
2 / 1

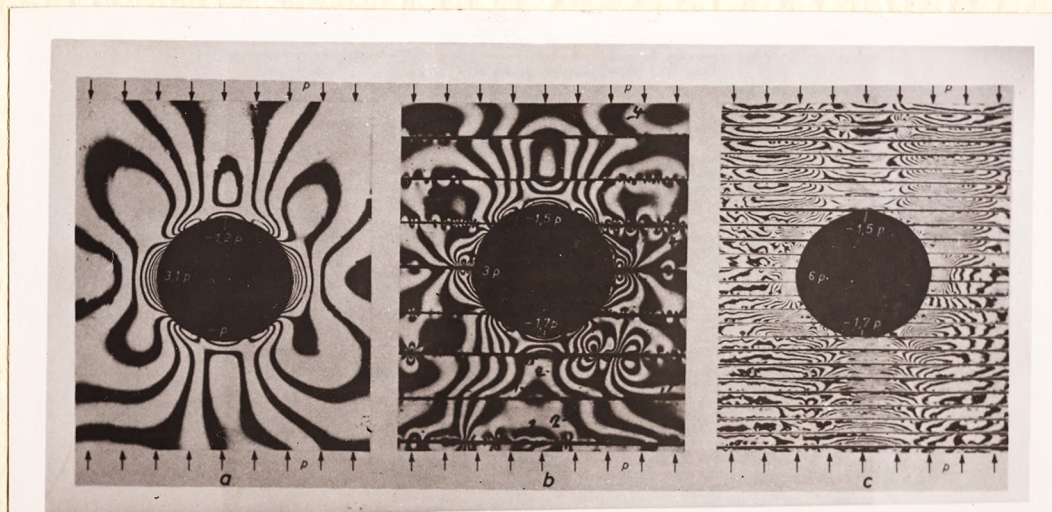
+ zone of compression, - zone of tension

Figure 1

Stress distribution
around openings
(after Dorstewitz)



Picture 1. Influence of Strata Bedding and Friction between Bedding on the Stress Distribution around Rectangular Openings.



Picture 2. Influence of Strata Bedding and Friction between Bedding on the Stress Distribution around Circular Openings (after Sonntag)

method, since the original and readjusted stress distribution is influenced only by the excavation process of the opening itself. The only significant strata movement is the deflection of the immediate roof above the opening.

Unsymmetrical Case : Openings in the Long Wall Mining Method

The study of stresses and movements around the headings and gate-roads driven on each side of the long wall face is much more complicated than in the case of room and pillar mining. Since the investigation of this strata behavior is rather new and of primary interest to the present model study, an intensive review of literature was necessary.

Additional Pressure. An advancing long wall face, single unit*, with the gate-roads A and B is shown in Figure 2. The stress distribution and the distortion of the strata in the neighborhood of these openings are heavily influenced by extraction of the coal on only one side of the gate-roads. Even if a flat formation is con-

*A mining operation with only one long wall and two gate-roads is defined as a "single unit". In a double or T-unit two long walls and three gate-roads are combined in one mining operation. In the center or haulage gate-road, the coal is extracted on both sides and a high distortion of the strata results.

sidered, the case becomes "unsymmetrical" under these conditions.

SONNTAG⁽⁹⁾ made photo-elastic studies with models representing the section C - C' in Figure 2 across the long wall face and obtained results as shown in the Pictures 3, 4 and 5. He considered an operation with full stowing and varied the thickness of the strata beds and the friction between them.

The strata behavior causes an additional pressure ahead of the working face, which is transferred to the gate-roads on either side. CREUELS and HERMES⁽¹⁰⁾ in the Netherland measured an increase of pressure in the long wall headings starting more than 600 feet ahead of the face and reaching a maximum when the face passed the measuring point. The total pressure reached in this case was from 1,125 to 5,312 psi. In Figure 3, the findings of JACOBI⁽¹¹⁾, who made similar investigation in Germany, are plotted. Since the depth here was almost twice as great as in the first example the pressures ranged from 2,500 to 14,250 psi. STASSEN and LIEGOIS⁽¹²⁾ in Belgium and SCHWARTZ^(13, 14) and DUBOIS⁽¹⁵⁾ in France obtained very similar results. They installed instruments in headings to measure the convergence of the hanging and foot walls, a factor dependent on the pressure, while the long wall face was (a) approaching, (b) passing and (c) moving away from the measuring points. The curve in Figure 4 shows the relation between the convergence (ordinate) and the time or distance* from the face (abscissa). The point of inflection I of this

*The relation between time and distance is given by the rate of advance of the long wall, i.e. 5 feet/day.

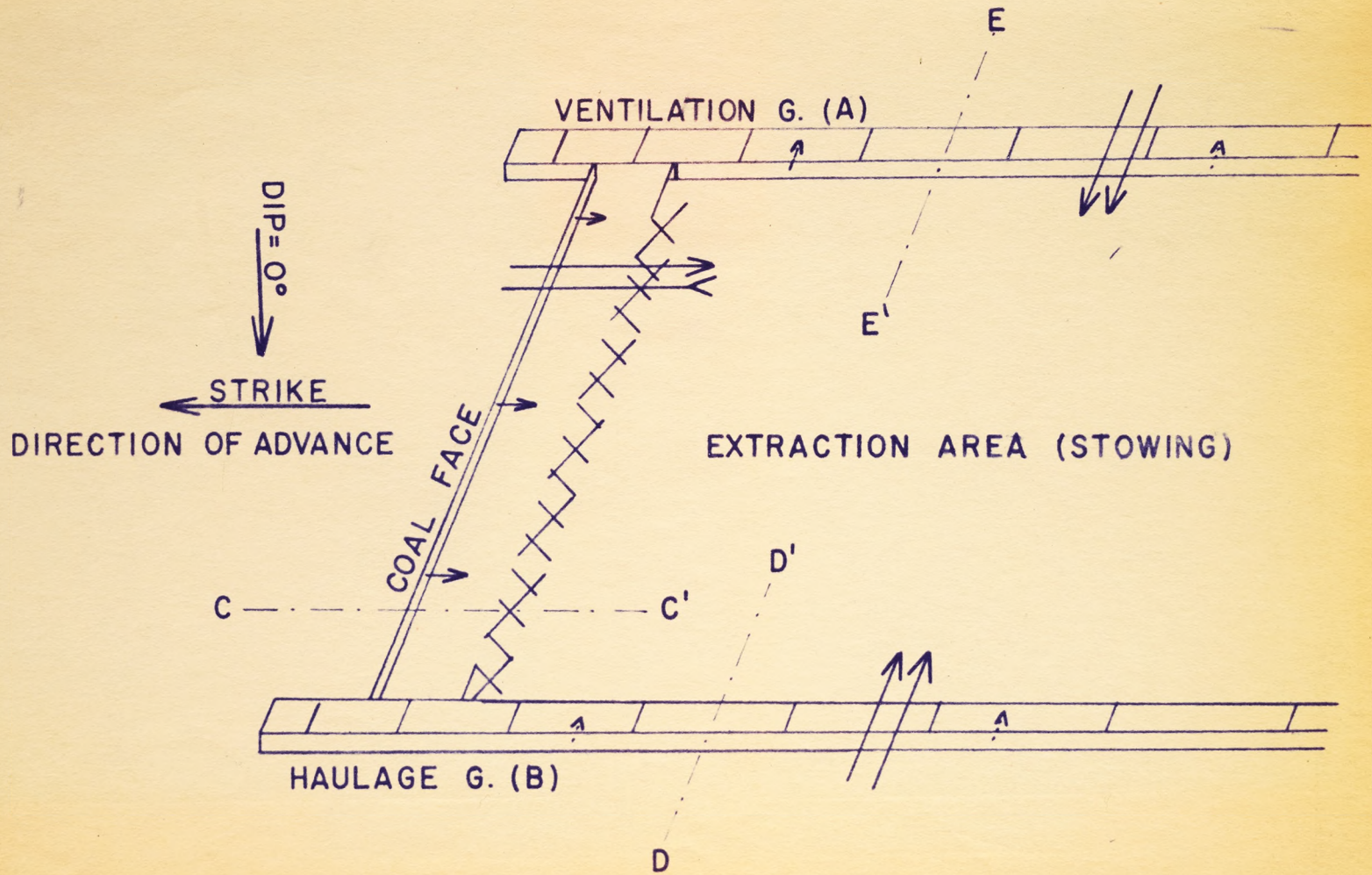
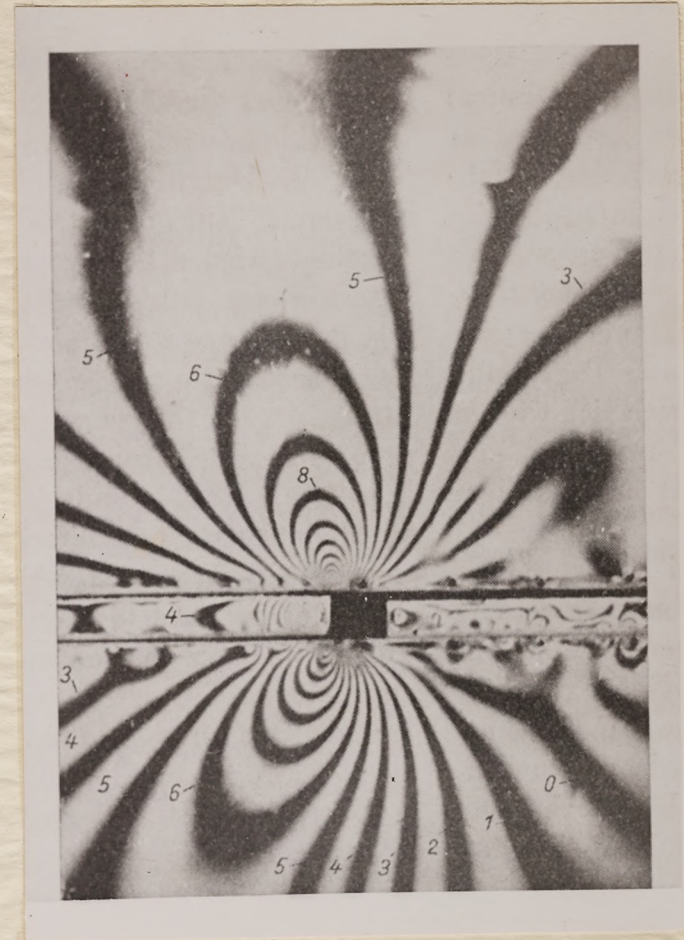


Figure 2

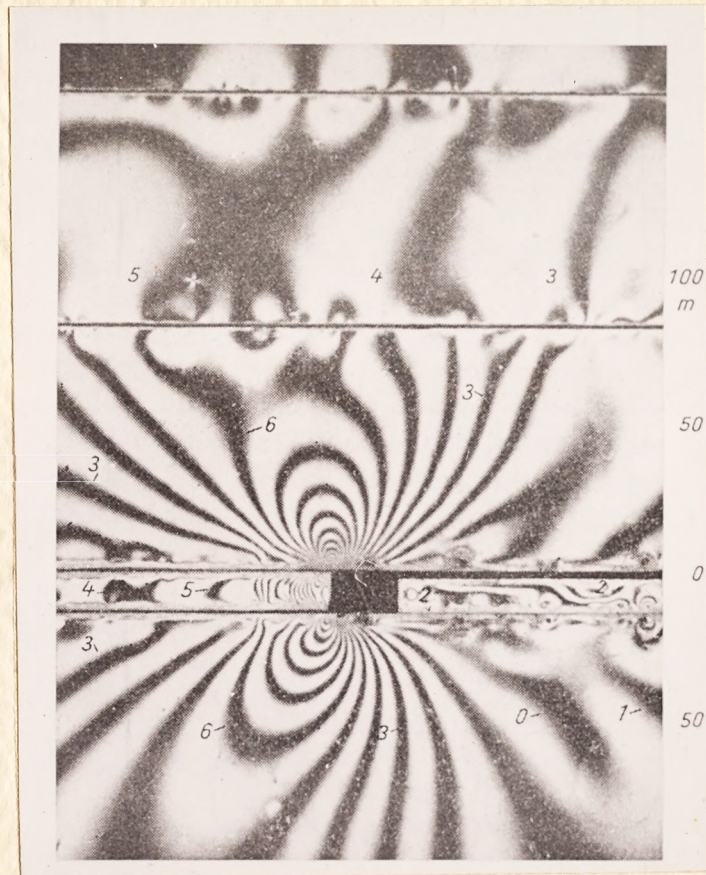
Schematic View of a Long Wall Operation



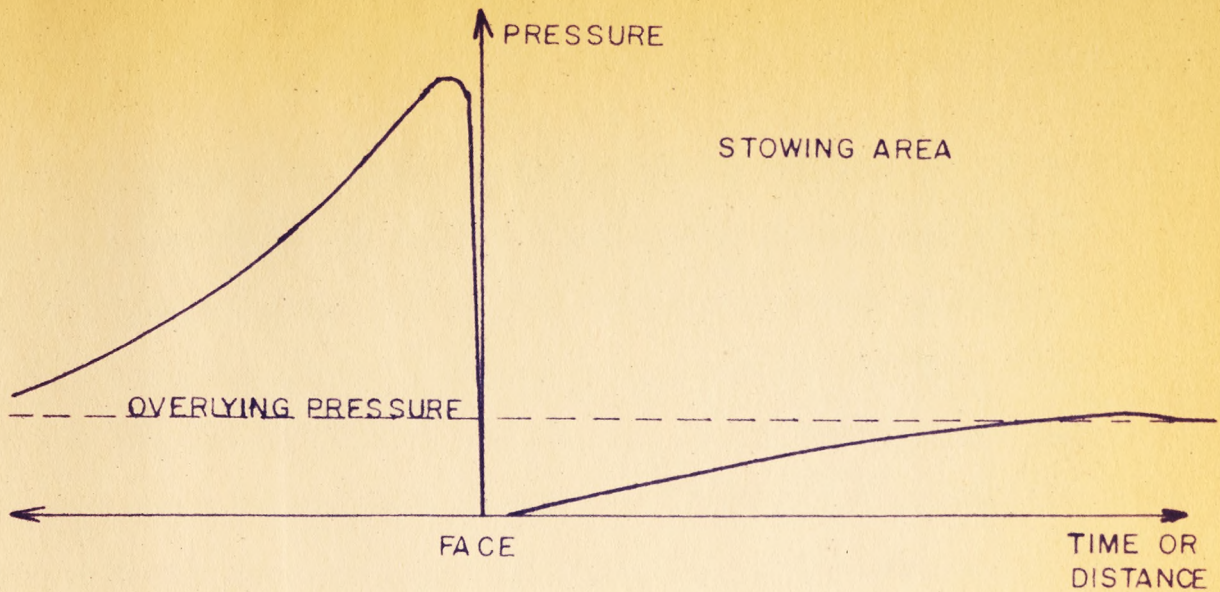
Picture 3. Stress Distribution in the Surroundings of a Long Wall Operation with thick Beds (after Sonntag)



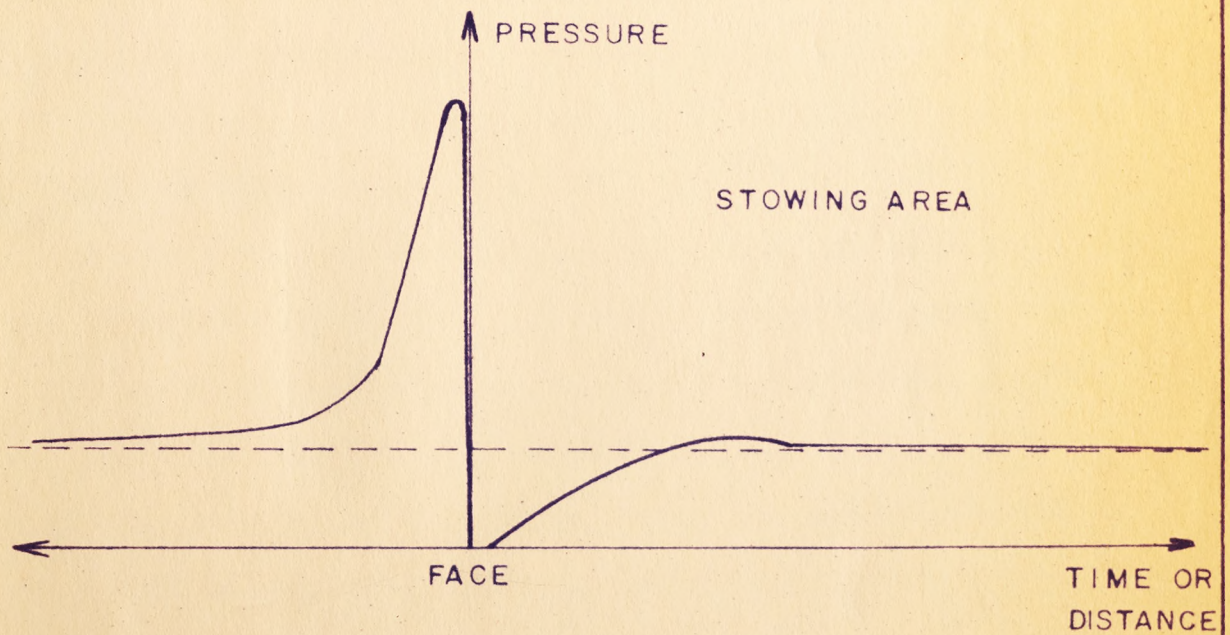
Picture 4. Stress Distribution in the Surroundings of a Long Wall Operation with low Friction between the Beds (after Sonntag)



Picture 5. Stress Distribution in the Surroundings of a Long Wall Operation with thinner Beds (after Sonntag)



(a) Strata with thick beds



(b) Strata with thin beds

Figure 3

Pressure "wave" accompanying
an advancing long wall

(after Sonntag and Jacobi)

so-called "S" - curve lies, dependent on the hardness of the strata and the seam (a) in the stowing area, (b) in the working area or (c) ahead of the face (Figure 5). During the course of these measurements the pressure reached its maximum 10 - 20 feet ahead of the face and was found to be as much as 4.5 times higher than the pressure P of the overlying strata (JACOBI)⁽¹¹⁾. When failure occurs in the coal seam near the face, the pressure drops down to almost zero in the distressed zone around the working room. By means of a specially designed measuring instrument, Jacobi followed the pressure in the stowing area and found a slow increase there, finally reaching a value as high as that due to the overlying strata. There was no indication of the occurrence of an abutment similar to that ahead of the long wall face (ATCINSON⁽¹⁶⁾)*.

The pressure wave accompanying the moving long wall face, which was also measured by HILBIG⁽¹⁷⁾, gives an idea of the extent to which the gate-roads are influenced by the advancing extraction process. Since the outer sides of the gate-roads (D and E in Figure 2), where the coal is left in its original position, also act like abutments with respect to the extraction area, the stress distribution becomes even more complicated.

*In the application of the "dome-theory" as a solution for the strata behavior above long wall operations, a second abutment far back in the stowing area was expected. The "trough-theory" after LEHMANN, which was confirmed by HILBIG⁽¹⁷⁾, agrees better with the actual measuring results obtained by Jacobi.

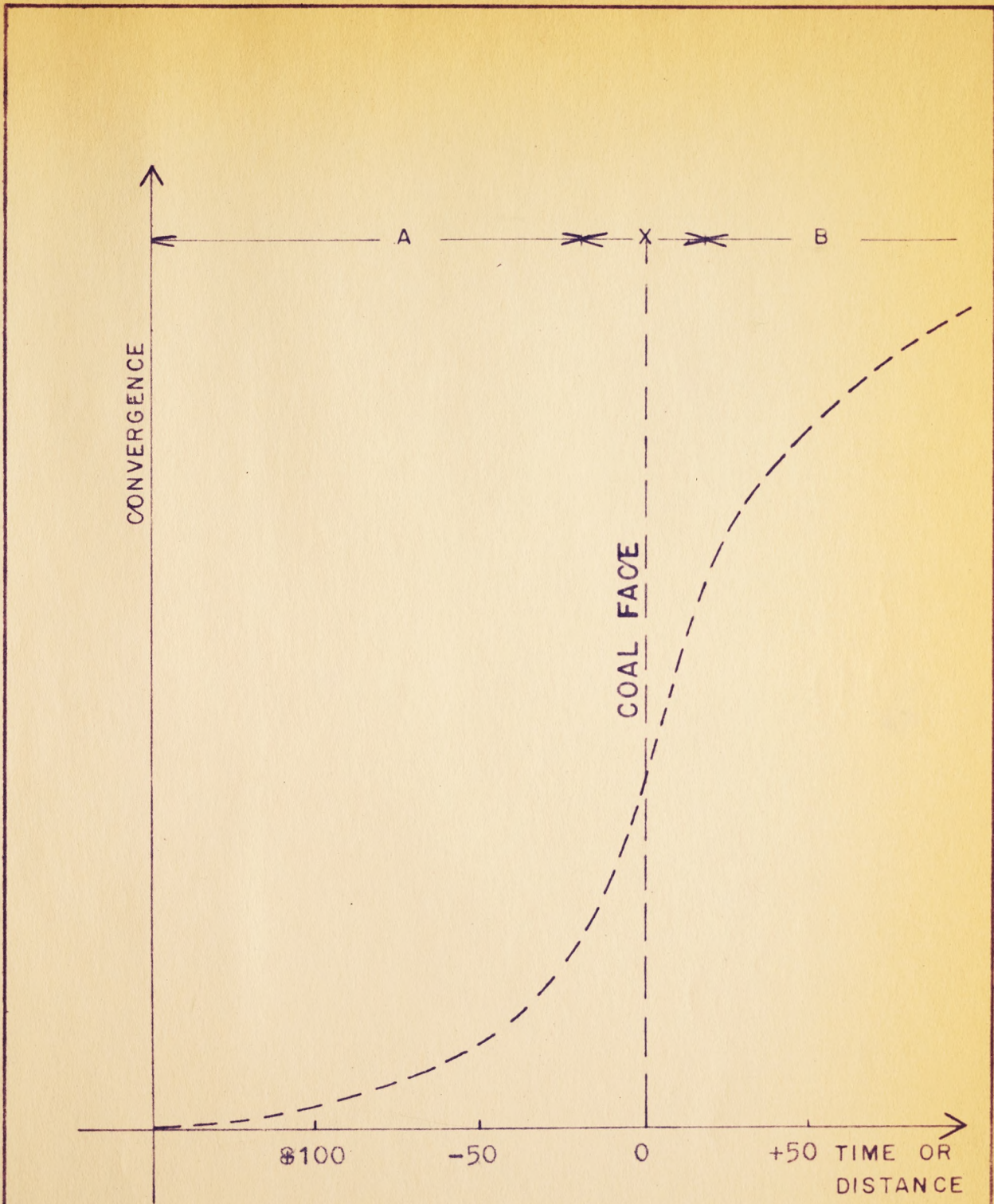


Figure 4 A ahead of the face " S " -curve
 X working area
 B stowing area

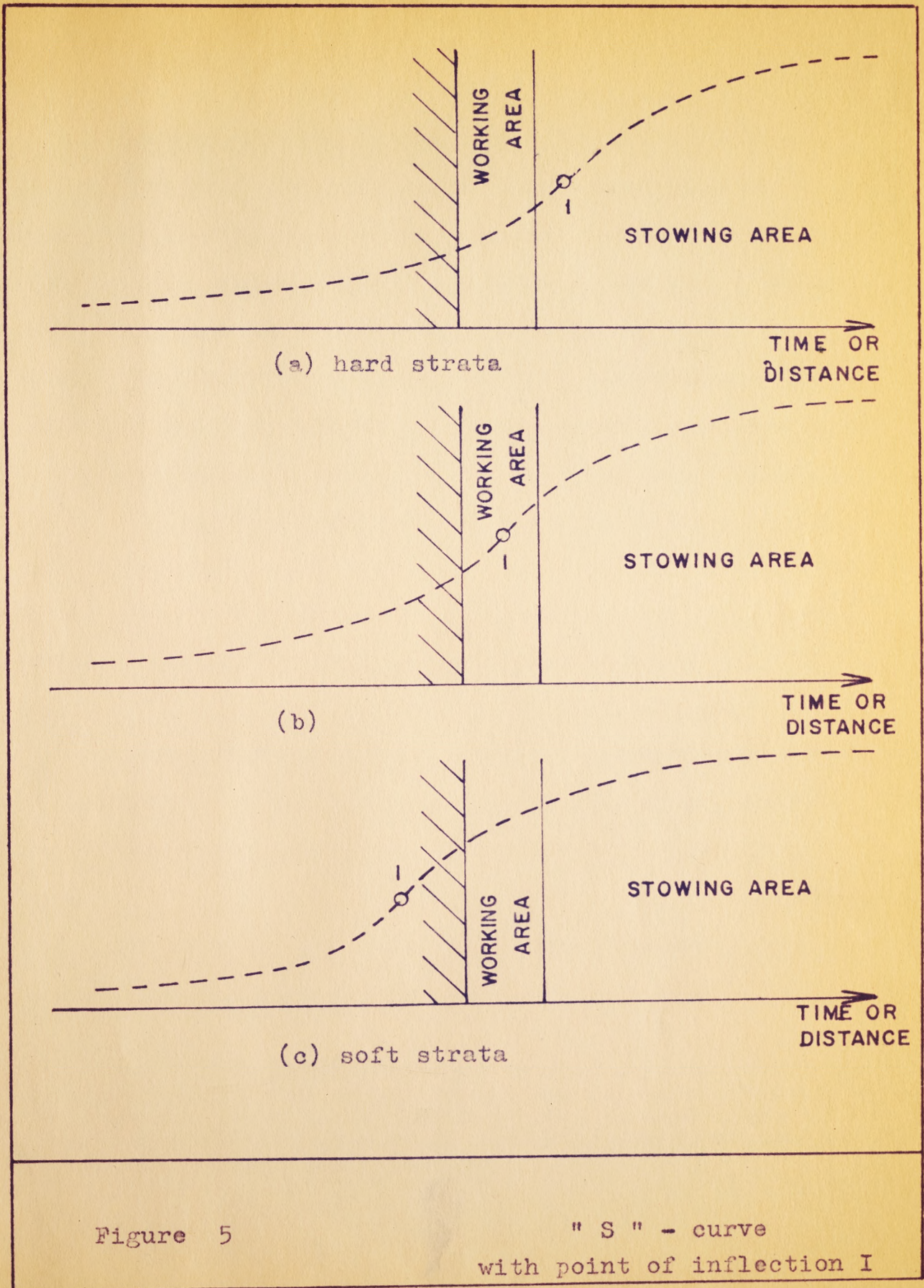


Figure 5

"S" - curve
with point of inflection I

(after Dubois)

Relaxation Movements of the Strata. Due to the additional pressure* described in the previous section, several kinds of strata movement can be observed, which do not occur in the neighborhood of openings under symmetrical loading conditions. The most significant movement is the convergence between the hanging and foot walls when the coal is extracted on one side. FLAKE⁽¹⁸⁾ made extensive investigations in this field and showed as a result, that the strata behavior perpendicular to the gate-roads (section D-D' and E-E' in Figure 2) is similar to that across the long wall working (section C-C' in the same figure). The amount of the convergence is dependent on the strength of the rock, the rate of advance and the compressibility of the stowing. These latter statements made by HOFFMANN⁽¹⁹⁾, GRAEBSCH⁽²⁰⁾ et al. were confirmed by the results of Flake.

According to MIDDENDORF and JACOBI⁽²¹⁾, HOEVELS and ROLSHOVEN⁽²²⁾ and KRIPPNER⁽²³⁾ et al., the relaxation movements of the strata in the neighborhood of gate-roads can be summarized in 5 significant points:

(1) Due to the coal extraction, a closure between hanging and foot walls can be observed. This convergence is not only dependent

*The amount of the additional pressure is naturally dependent on the convergence in the total mining region. The convergence, however, can be controlled to a certain extent by the method of stowing or caving, which influences the strata movements in the long wall area and around gate-roads considerably.

on the thickness of the seam but also on other factors, such as, the strength of the strata, the support resistance and the yielding rate of the cribs or checks on the extraction side (D' or E' in Figure 2). The radius of deflection of the strata which influences the shape of the convergence curve is much larger for sandstone than for clayey shale*, both in the hanging and foot walls.

(2) Along the axes of the gate-roads, the hanging and foot walls move in opposite directions; the hanging wall being drawn towards the stowing area. The amount of these movements is again dependent on the strength of the rock. Measurements of strain in connection with these movements lead to the assumption that sandstone behaves elastically under these circumstances, while clayey shale shows large deformations which are not recoverable. Particular reference to this occurrence is given by SCHUERMAN⁽²⁴⁾.

(3) Perpendicular to the long axes of the gate-roads in the plane of section D-D' in Figure 2, both hanging and foot wall move towards the extraction area. These displacements were also found to be dependent on the type of the associated rock and according to GRAEBSCH⁽¹⁹⁾ approximately twice as great for sandstone as for sand shale.

*Sandstone, shale and clayey shale are the predominate country rocks in coal depositions.

(4) Both hanging and foot wall show a bed separation as a result of the strata movements, cited under (1) to (3). This occurrence is favored in particular by the bed displacements in the lateral directions, (2). The amount of bed defoliation increases with the decrease in strata strength; sandstone exhibiting less separation than shale (GRAEBSCH⁽²⁰⁾).

(5) The gate-road walls move towards the openings as a result of the general movement of the rock mass into the stowing area, as well as the additional pressure developed during the opening extraction process (18, 19, 20 and 21).

Theory and Practice of Roof Bolting in Stratified Rock

Any support underground should preserve the original size and shape of the opening for haulage and ventilation (FRITZSCHE⁽²⁵⁾ LEWIS⁽²⁶⁾). With an increase in depth this objective becomes more difficult to attain, due to the increase in the vertical pressure resulting from the overlying strata. Differences between the properties of rock types encountered also become more important. As long as the induced stresses do not exceed the strength of the rock around the opening, large distortions will not occur. If, however, the material is originally weak, or if the strength is diminished by blasting or weathering effects, failure may be observed. A zone of distressed rock

will form around the opening and load the man-made supports by its weight.

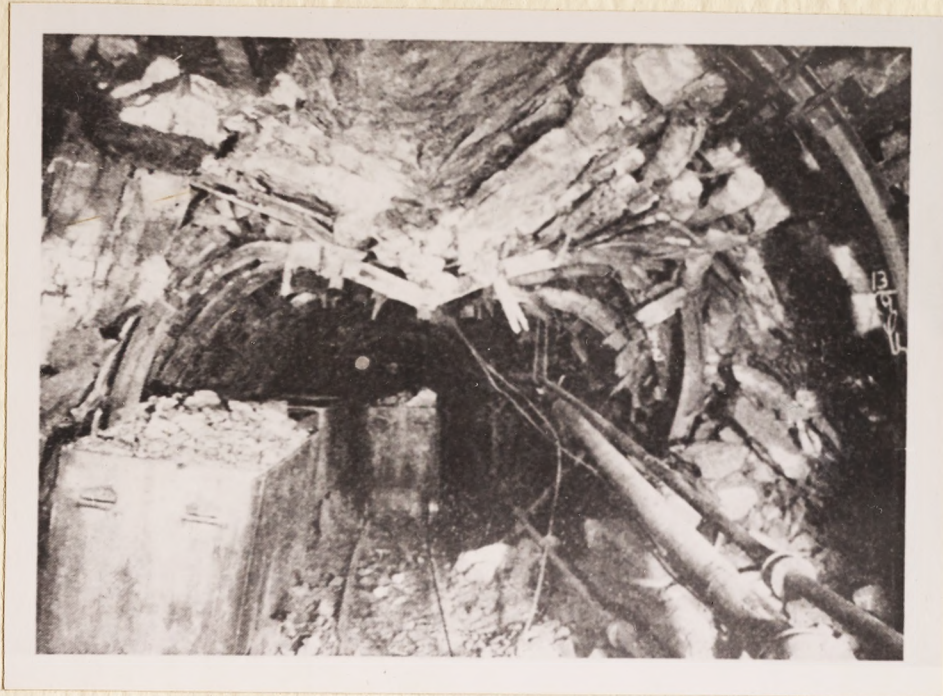
If a new equilibrium is not achieved within a short distance from the wall of the opening, the destressing process continues in the zone between the support and the effective stress ellipse, and a pseudo-plastic behavior of the strata will be seen (Picture 6).

SCHUERMAN^(24, 27) stated that these pseudo-plastic movements can only occur, when the elastic strength of the rock is exceeded and the rock tries to reach a new state of equilibrium. With an extension of the distressed zone, the weight on the artificial support will increase and for this reason this zone should be kept as small as possible.

If the convergence of the overlying strata is considered in addition to the pseudo-plastic behavior of the adjacent strata, two major criteria for any support are:

- (a) development of high reinforcement to reduce bed separation and to keep the distressed zone small,
- (b) a built-in yielding effect to prevent unwanted deformation and distortion of the support, since a certain amount of convergence cannot be avoided.

It is normally not possible to fulfill both requirements by conventional support, since the reinforcing and yielding effect contradict to a certain extent. To stabilize the strata around an opening, an improve-



Picture 6. Pseudo-plastic Behavior of the Strata in a Long Wall Gate-road.



Picture 7. "Quarter-Moon" Shape in a Borehole caused by Bed Displacement.

ment can be achieved by the application of roof bolts based on several effects, which may be divided into two groups:

- (a) The securing of material which has already failed,
- (b) The prevention of failure and decrease of the relaxation movements.

Both effects are discussed theoretically and explained in the literature as follows:

Suspension Theory

Roof bolts may be used to secure fractured pieces of the strata to solid ground. Since the bolts must support the full load of any rock fragment which may come against it, sufficient strength and anchorage is required to support the estimated weight of the largest piece it may have to hold (THOMAS⁽²⁸⁾). SCHMUCK⁽²⁹⁾ cited an example in a Colorado coal mine, where 1-inch wedge type bolts of only 24 inches length were used to tie a thin band of shale to a sandstone above. BUCKY⁽³⁰⁾ and JACOBI⁽³¹⁾ calculated the suspension effect of roof bolts for static loading conditions. According to the latter author, the weight of a bed for one meter length of roadway was 11,25 tons, based on the following data:

span of the opening	= 4,5 m
thickness of the bed	= 1,0 m
specific gravity	= 2,5 tons/m ³

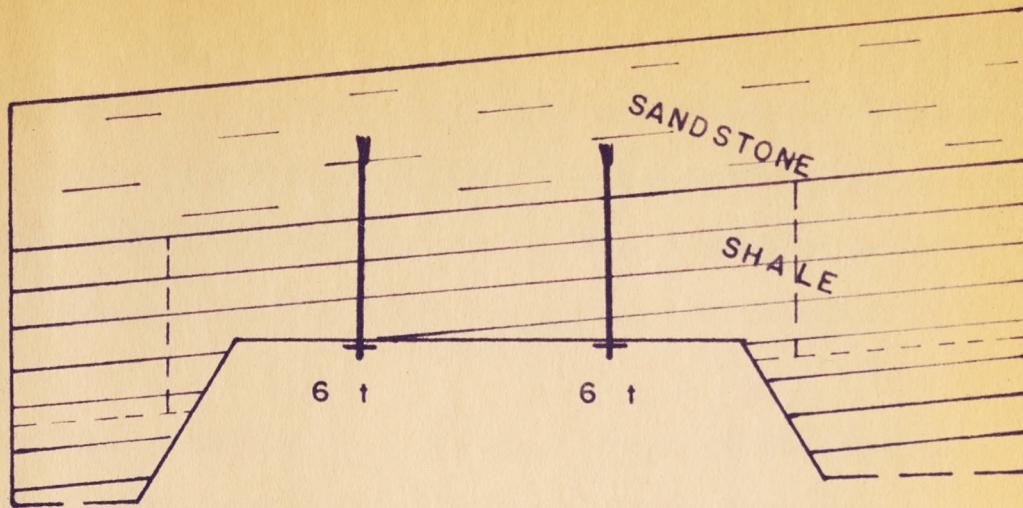


Figure 6

Two roof bolts as suspension support

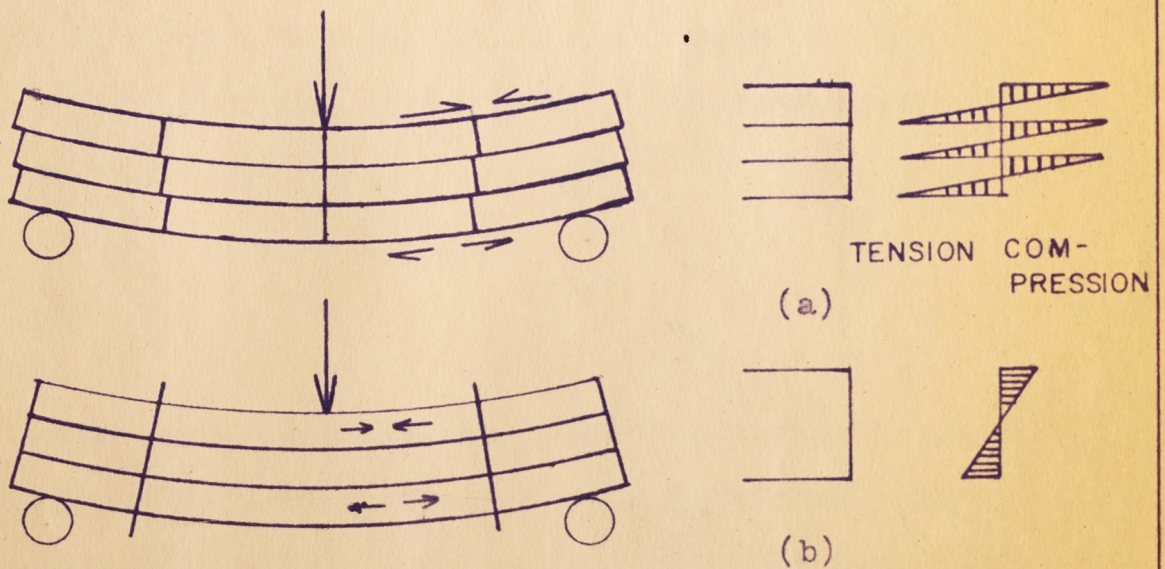


Figure 7

"Plug-effect" of roof bolts

Two bolts with a load capacity of 6 tons each would be sufficient to suspend the bed (Figure 6). The actual load can be considered to be even less, since the ends of the beam or plate might be supported to a certain extent. For this example the following assumptions were made:

- (a) The existence of sufficient strength of the sandstone in tension and compression for the anchorage of the bolt heads.
- (b) Negligible deflection of the main roof.
- (c) No distortion of the clay by weathering.
- (d) No indenting of the washers into the clay under a load of 6 tons.

The suspension conditions as given in the example by Jacobi have been confirmed by other authors, and can be applied also to a higher number of bolts where the dimensions and weight, respectively, of the suspended rock increases.

Beam Theory

In many cases, geological conditions will exclude the possibilities of suspension of the immediate roof, either because a stronger bed does not exist or is so high above the opening that an economical use of bolts is out of question. Besides the strength of the rock, thickness of the beds is a contributing factor to the stability of the strata around the opening. In 1952, JACOBI⁽³¹⁾ calculated, as an

example, that a bed of 33 cm thickness with a tensile strength of 5 kg/cm^2 , a compressive strength of 100 kg/cm^2 and a span of 5 meters could just support its own weight. A thinner beam would break under the same conditions, while a thicker one would carry more load. Similar calculations were made by OBERT, DUVALL and MERILL⁽⁵⁾ in 1960, who also developed several formulas for the relationships between these pertinent factors.

The thickness of the effective beam can be increased by clamping several thinner layers together with the aid of roof bolts.

KRIPPNER⁽²³⁾ and JACOBI⁽³¹⁾ compared the bending strength and the deflection of three boards for two cases: (a) with nails and (b) without nails, the nails representing the effect of the bolts.

(Figure 7). If elastic behavior and the same load are assumed in both cases, stresses are diminished to $1/3$ and deflection to $1/9$ in case (b) as compared to (a). The load capacity is three times higher and with this increased load the deflection is only $1/3$.

PANEK⁽³²⁾ in 1956, introduced the laws of mechanics into the discussion concerning roof bolt application in stratified rock and expressed the maximum bending and shearing stress of the rock beam above an opening underground as

$$\sigma_{x(\max)} = \frac{wL^2}{2t} \quad (1)$$

$$\tau_{xy(\max)} = \frac{3wL}{4} \quad (2)$$

The deflection at mid span was determined as

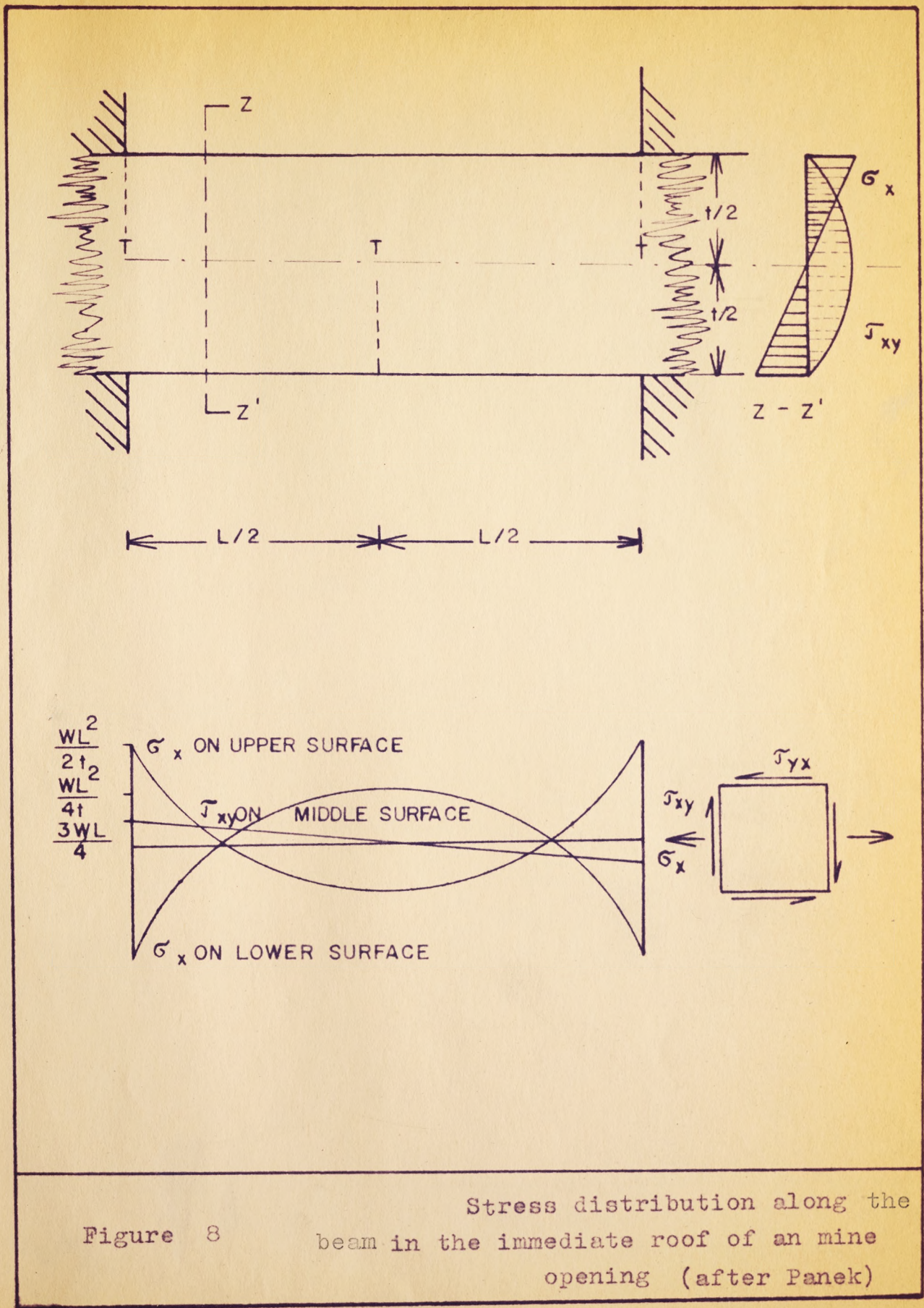
$$\delta = \frac{WL^4}{32Et^2} \quad (3)$$

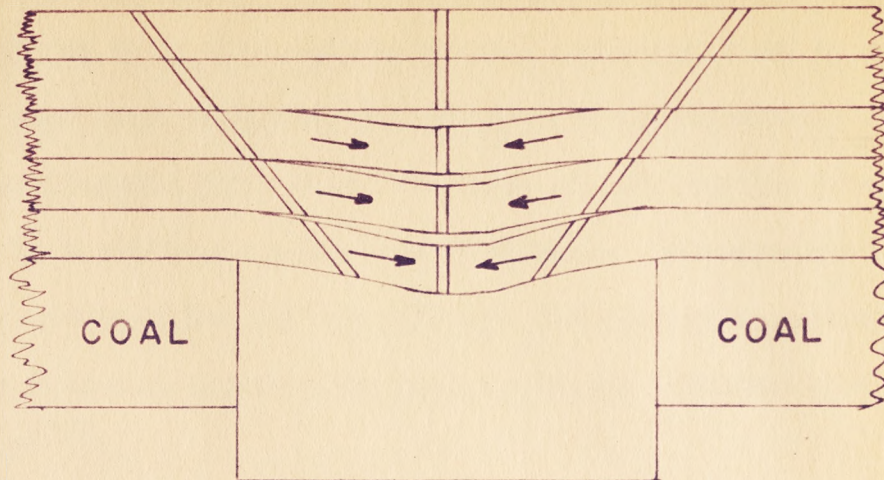
- t = thickness of the beam,
 L = span of the opening,
 W = weight per unit volume,
 E = modulus of elasticity.

The reciprocal relationship between the maximum bending stress σ_x and the thickness of the beam t is expressed in equation (1), σ_x ordinarily being much greater than the shearing stress. The stress distribution along the beam is shown in Figure 8.

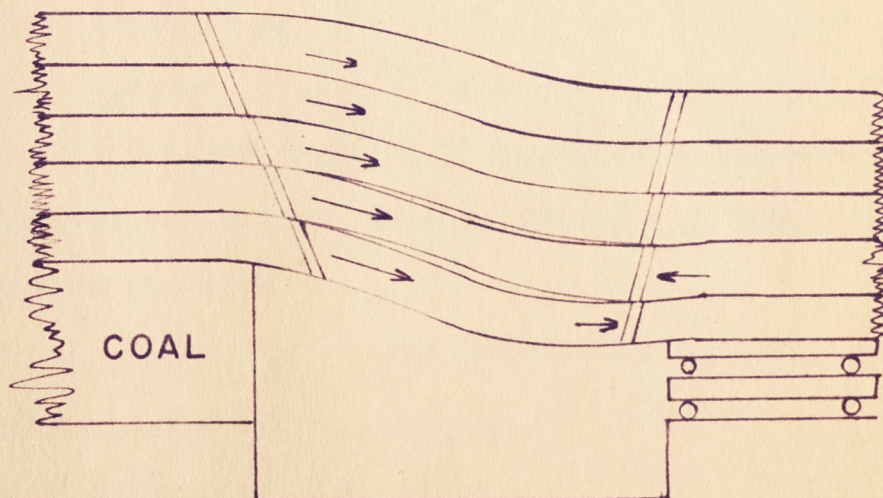
Several adjacent individual beds of equal thickness and modulus of elasticity do not influence one another and individually develop the same stresses and deflections as a single beam. MIDDENDORF⁽²⁰⁾ and JACOBI⁽²¹⁾ and SCHUERMANN⁽²⁷⁾ investigated bed displacements by drilling vertical and inclined holes into the immediate roof of openings without installing bolts. The results, after a period of settlement, are summarized schematically in Figure 9 for the symmetrical and unsymmetrical cases. A view inside a borehole shows the occurrence of the typical "quarter moon" shape due to the relative bed displacements (Picture 7).

To decrease the displacement, deflection and stress and to increase the effective thickness of the working beam, roof bolts can be installed; their action being based on four different effects.





(a) Symmetrical case



(b) Unsymmetrical case

Increase of Frictional Resistance to Bedding-plane Slip. As shown in Figure 9, a slip occurs between different beds in the immediate roof when pressure is applied. If gravitational load is assumed for a symmetrical case, the slip at mid span is zero and increases to a maximum towards the abutments. In unsymmetrical cases, the distribution of the relative displacements occurring when the static friction between the beds is exceeded becomes more complex (PANEK⁽³³⁾).

If roof bolts are installed with pre-tension, the slip and the deflection can be reduced due to the higher friction force developed. The bolt effect for this type of reinforcement, is of particular interest near both sides of the opening, where the largest relative displacement is found. JACOBI⁽³¹⁾ calculated, for a symmetrical example, that a friction force of 35 tons between two beds of 0,5 m thickness was needed on each side, to prevent any deflection. The supporting data given were:

load	=	3,0 m of strata
specific gravity	=	2,5 tons/m ³
span of the opening	=	5,0 m
compressive strength	=	200 kg/cm ²
tensile strength	=	10 kg/cm ²

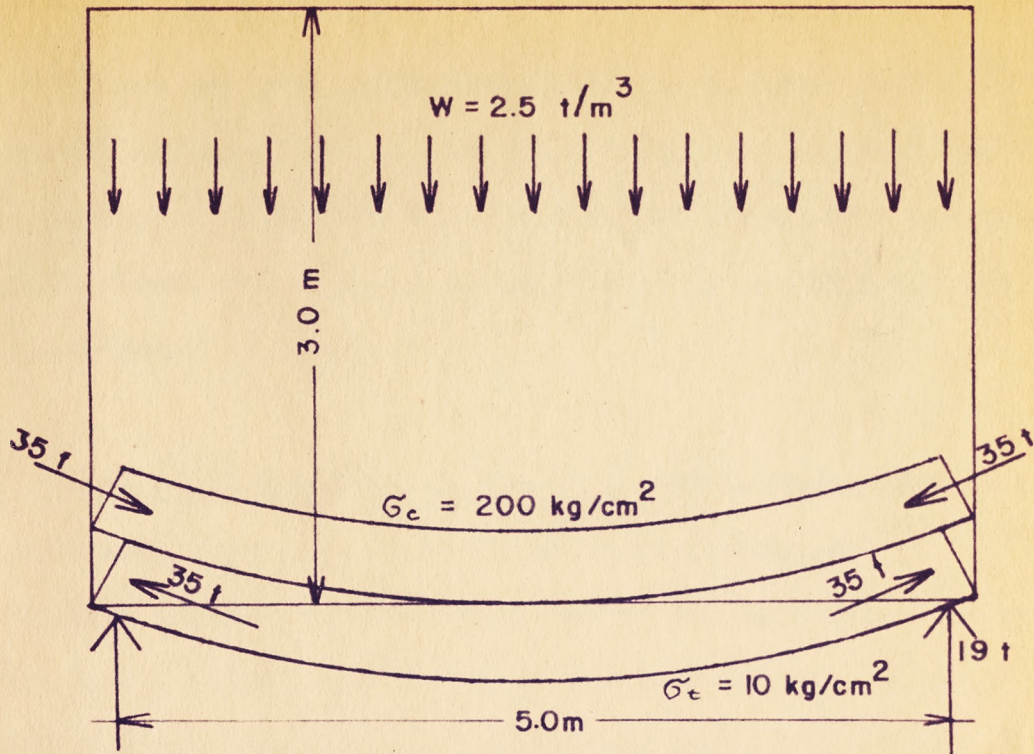
(See also Figure 10)

If a friction value of $\mu = 1,0$ for stone on stone is assumed, the

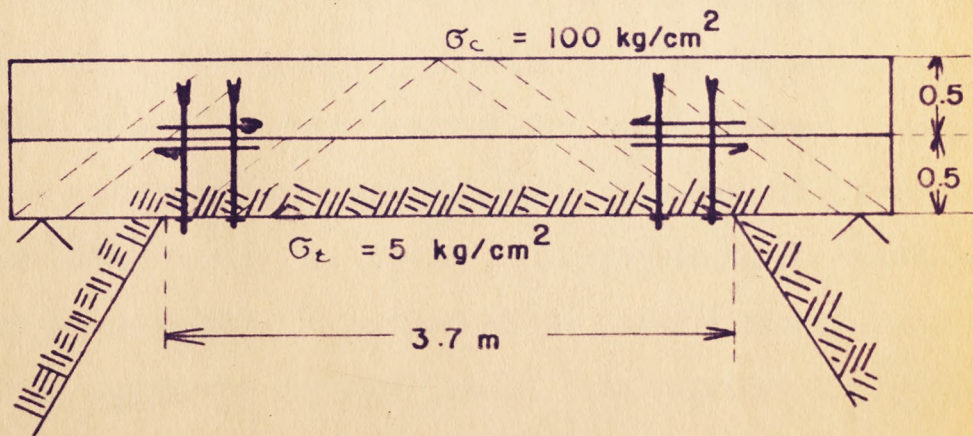
friction force of 35 tons can be achieved by 4 bolts, which must be tightened with a pre-tension of 17.5 tons each. As a conclusion it was stated by Jacobi that the friction increases in proportion to the pre-tension of the bolts.

Shear Strength of the Roof Bolts ("Plug" - Effect). Bedding-plane slip and deflection can also be decreased if roof bolts with high shear strength are installed (27, 31, 32, 33, 34 and 35). Even if the friction effect, discussed in the previous paragraph, is neglected, two steel bolts of 30 mm in diameter would be sufficient to prevent any slip or deflection; the stresses, however, around the bolt holes would be extremely high and might cause rock failure in the neighborhood of the bolts. With a small beam deflection due to slip, the "plug" - effect comes into action since the diameter of bolt and hole always differ slightly.

Shear Reinforcement in the Rock. Neither increase in frictional resistance nor the "plug" - effect can prevent rock failure in shear (30, 31, 32 and 35). If the rock tensile strength is sufficiently high, shear cracks will occur near both abutments when the load reaches a critical point. The beam may be assumed as a series of cubes whose vertical interplanes represent the planes of shear. Roof bolts installed at an angle of, i.e. 45° , through the shearing planes



(a) Without bolts



(b) With 4 bolts

Figure 10

Increase of frictional resistance
to bedding-plane slip by
roof bolts

(after Jacobi)

can reinforce the beam considerably (Figure 11 after JACOBI⁽³¹⁾). The strengthening effect of this bolt pattern is explained by the basic laws of a framework; the bolts act as hinged tie bars while diagonal struts are built up in the rock beam and thus the roof will be strengthened in shear.

Tensile Reinforcement in the Rock. Since most rocks in the carboniferous strata have a very low tensile strength^(18, 19 and 20), the bending stresses on the lower side of the beam should be transferred to a reinforcement. This can be done by connecting the bolt ends with wire ropes or steel bars at the lower side of the beam. It was calculated by JACOBI⁽³¹⁾ that the tensile stress developed in a beam might be carried completely by this kind of reinforcement, when a pre-tension of 23,3 tons in the wire could be applied. The data accompanying this example are the same as in the previous cases (Figure 12). The theoretical calculations must, however, be adjusted, since in an underground opening the acting abutments of a beam are beyond the walls, inside the pillars, and reinforcement cannot be mounted at these points. A portion of the tensile stresses must therefore be carried by the rock itself. The value of 3.2 kg/cm^2 in the given example is too small, since a very high pre-tension in the wire was assumed, which cannot be reached in actual practice underground.

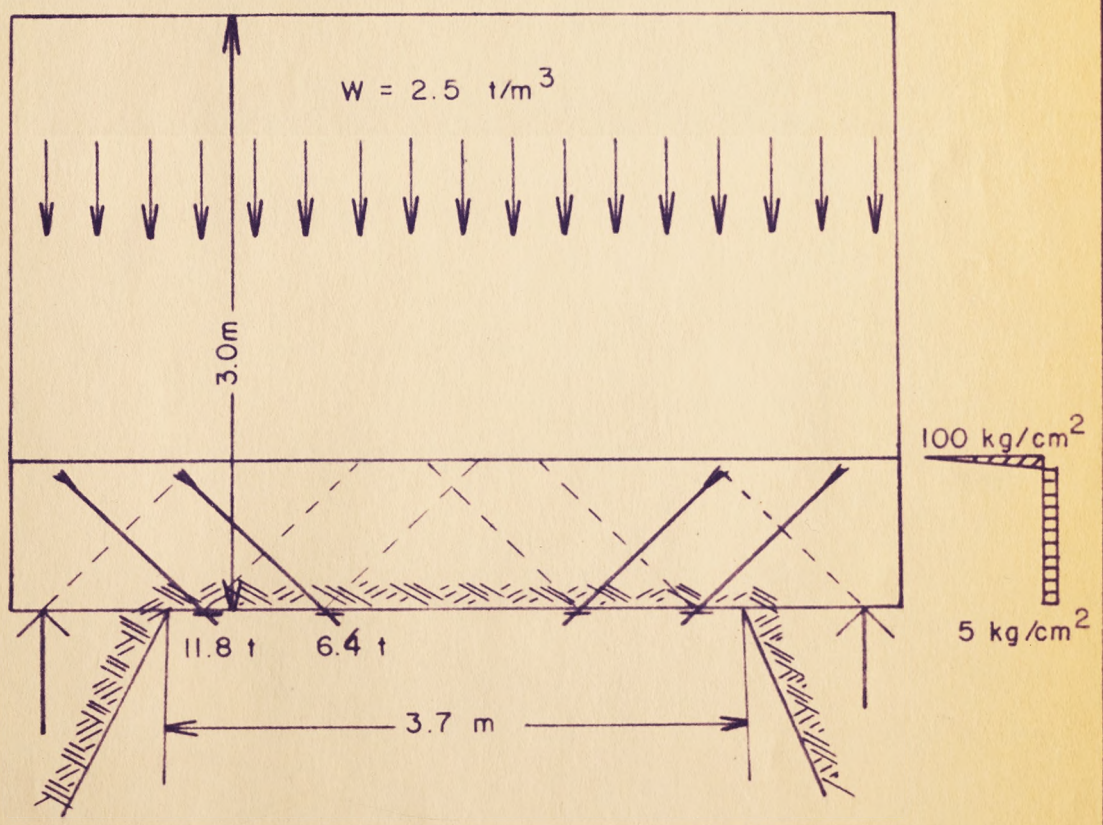
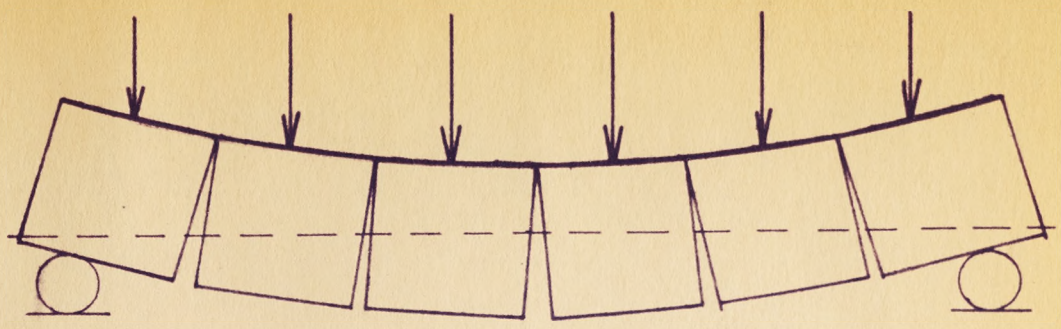
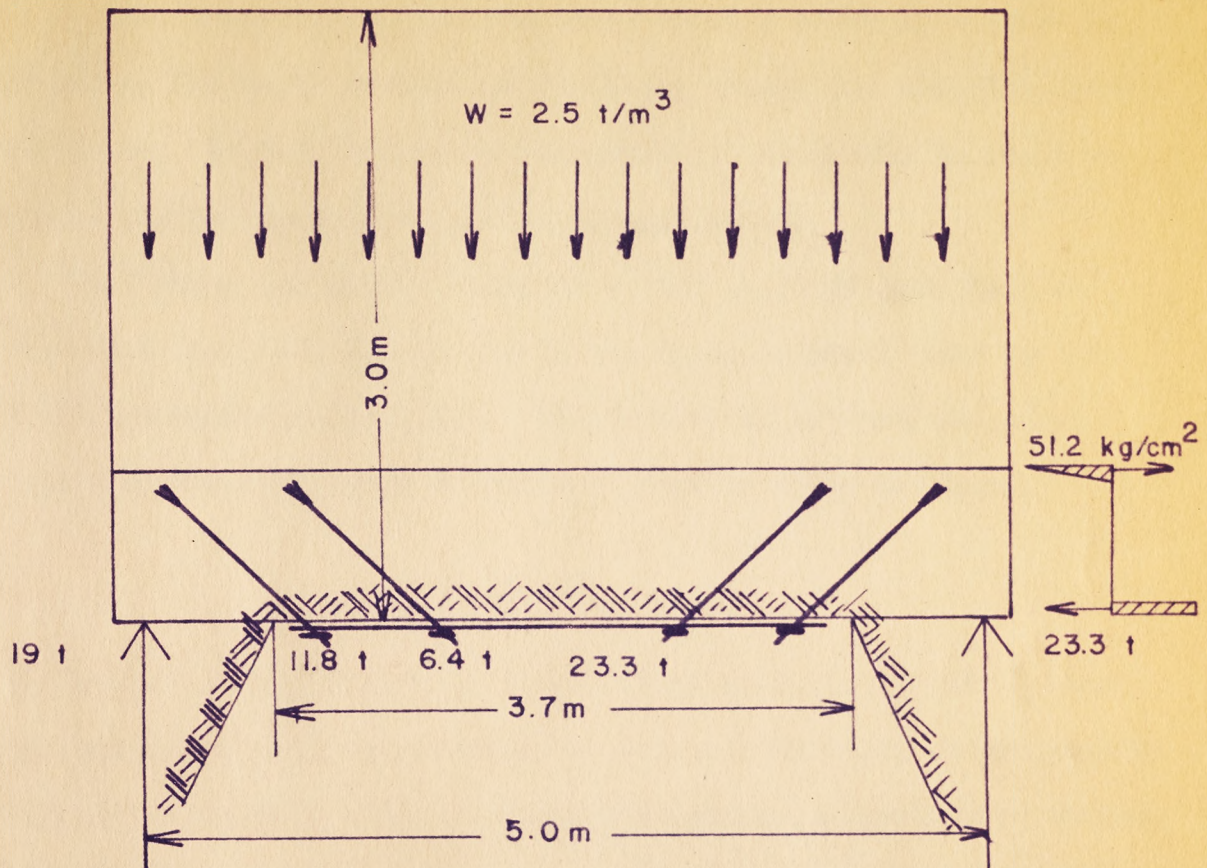


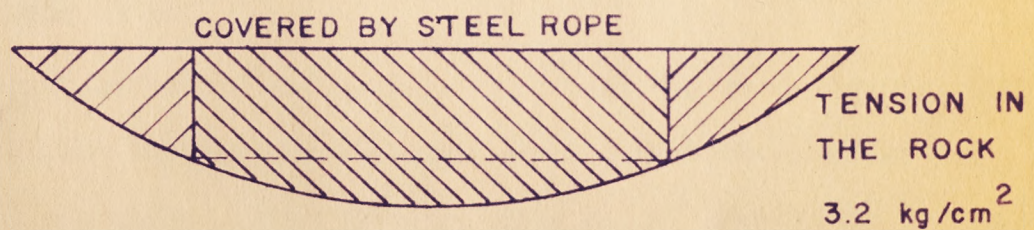
Figure 11

Shear reinforcement of the strata by roof bolts

(after Jacobi)



(a) Installation of 4 bolts and a wire rope



(b) Moment diagram

Figure 12

Tensile reinforcement of
the strata by roof bolts

(after Jacobi)

If a clamped beam is considered, the tensile stresses in the reinforcement device would be lower (JACOBI⁽³¹⁾). The remaining tensile stress, however, in the rock could cause a crack at either end, starting on the upper surface of the beam, making the clamping-action ineffective. In practice it is therefore not desirable to consider the roof strata around openings as clamped beams.

Roof bolts can be installed at a flat angle of less than 45° , to transfer the tensile stresses in the ropes or steel bars as far into the abutments as possible. The connection between the ropes or bars and the bolts must be strong enough to carry the load.

Model Study

To confirm the results of theoretical analysis of underground stress conditions and specifically to obtain additional information as to the effect of roof bolts on opening stability, experimental studies with small-size models have been performed by various investigators (21, 32-40).

Theory of Model Study

Stress distribution and stress magnitudes can be determined for actual conditions underground when the similitude between model and prototype is adequate. While in some tests visual observation of the model under load can give an indication of the behavior of the prototype, measurements of strain, deflection, etc., are required in more accurate investigations. To translate the results of these tests to a full-scale structure, it is necessary to consider the conditions for structural similarity between model and prototype which may be

derived from the equation of some quantity, such as the stress, at a given point in the structure (PANEK⁽⁴¹⁾). By dimensional analysis, a general equation can be obtained which must hold true for both model and prototype:

$$\frac{\sigma}{E} = f \left(\frac{AWL}{4}, \frac{P}{EL^2}, \frac{L}{t}, \frac{L}{b}, \frac{h}{t}, K, \frac{X}{L}, \frac{Y}{L}, \frac{Z}{L}, \frac{M}{PL}, F, \frac{d^o}{d}, \frac{d^o}{L}, \right. \\ \left. \frac{AW^o}{AW}, \frac{E^o}{E}, \gamma, \gamma^o \right) * \quad (4)$$

Model tests can be either destructive or nondestructive. In the first case it is possible to determine only certain maximum stresses which occur at the time of failure. In nondestructive tests, the state of strain in the model, and from this the similar condition in the prototype, can be indicated for any load below failure. In the latter case, the model can be constructed of materials different from that of the prototype and by measuring the model strains according to several load values, a load-strain relationship can be determined from a single test. The results, which consist in most cases of quantitative relations between the load, the strain and the dimensions and properties of the structural members, are directly applicable to any prototype that satisfies the similarity requirements.

* See Notation

Few model studies of openings in the neighborhood of long wall workings have been performed in the past, because of the difficulty in duplicating the loading conditions and the strata movements under unsymmetrical circumstances, which were described earlier in this chapter. It has been indicated by CAUDLE and CLARK⁽⁴²⁾ that there is negligible difference in the bending and shearing stresses in a symmetrical beam whether it is loaded by either a uniform load, its own weight or centrifugal forces. To imitate, however, the load distribution and the strata movement of an actual mine opening in a model for an unsymmetrical case, a device utilizing surface load is not adequate and therefore two methods providing the necessary body forces remain:

(a) the usage of low-strength material causing deflection in the model by its own weight (single body force). This effect might be observed with gelatine and paraffine, or perhaps a low-modulus epoxy resin plastic as recently developed by HABER⁽⁴³⁾.

(b) a controlled increase of the body forces in the model material.

A centrifuge provides one facility for the second method and permits experiments independent of the material properties (BUCKY⁽⁴⁷⁾, PANEK^(33, 34, 35, 41), DALLY, DURELLI and RILEY⁽⁴⁴⁾, HOEK and BERNER⁽⁴⁵⁾, HOEK⁽⁴⁶⁾). The centrifugal acceleration has the effect of increasing the effective weight per unit volume of the material, thereby satis-

fying the model-prototype similarity conditions formulated by PANEK⁽⁴¹⁾, who has shown that centrifugal testing can be used for accurate analysis of body force problems. Similitude equations can be established for the dimensions and properties of the model and the prototype, such as,

$$L_m = \frac{1}{S} L_p \quad (5)$$

$$W_m = S \frac{E_m}{E_p} W_p \quad (6)$$

Where S is the model-prototype scale factor

To obtain an effective weight of the model corresponding to a chosen scale factor S, the speed of the centrifuge can be controlled such that A, the ratio of the gravitational load w and the centrifugal load Z, coincides with S.

$$W_{\text{eff } m} = \frac{E_m}{E_p} A W_m = \frac{E_m}{E_p} S W_p \quad \text{or} \quad A = \frac{E_m}{E_p} \frac{W_p}{W_m} S \quad (7)$$

$$\text{Gravitational load } w = m g \quad (8)$$

m = unit mass

g = acceleration due to gravity

$$\text{Centrifugal load } Z = \frac{m}{g} \frac{v^2}{R} \quad (9)$$

$$v = R\omega = \text{velocity}$$

$$R = \text{radius of the rotor}$$

$$\omega = 2\pi N$$

$$N = \text{R.P.M.}$$

$$\text{Ratio } A = Z/w = \frac{v^2}{gR} \quad (10)$$

$$A = \frac{4\pi^2 RN^2}{g}$$

The factor A is a measure of what number of "g's" is developed in the test, that is, what body force is applied in comparison to the weight of the model.

Photo-elasticity as Applied to Model Study (FROCHT⁽⁴⁹⁾)

The theory of elasticity is a very powerful tool for solving stress problems but the mathematical difficulties involved in its use increase when the shape of the investigated structure and the load applied to it become complex. Under these conditions, one may resort to experimental methods, of which photo-elasticity used in connection with models is a very simple and suitable one.

In recent years, the development of new synthetic resins which possess photo-elastic properties has led to modern model studies in the field of experimental stress analysis. A series of colored bands are observed in the model while under load when viewed by transmitted white light or alternate dark and bright bands called "fringes" when using monochromatic light. Analysis of these stress-optical effects gives the distribution of the stresses acting within the model. The stresses in the small photo-elastic models used are directly proportional to the stresses in the prototype, if model and prototype are loaded below their respective elastic limits and if similitude conditions governing multi-material structures are obeyed (PANEK⁽⁴¹⁾).

For the analysis of photo-elastic effects in model studies, the use of circularly polarized light is convenient. When the transverse vibrations of a light ray are confined to parallel planes, the light is said to be plane polarized. Either white or monochromatic light can be plane polarized. When two of these light waves having the same amplitude and frequency vibrate at right angles and a quarter of a wave length out of phase circularly polarized light is obtained. This effect can be obtained by passing plane polarized light through a so-called quarter wave plate which consists of a bi-refringent material such as mica. When light falls on the plate at normal incidence it is resolved along two component planes at right

angles and because the optical properties on the two planes are different, the two components are transmitted with different velocities. When they emerge from the plate, there is a difference in phase between the waves, which is proportional to the thickness of the plate. If this thickness is such that the relative phase displacement of the light of a given wave length is one quarter of a wave length, then the plate is known as a "quarter-wave" plate.

Almost all transparent materials, such as glass, celluloid and certain plastics become bi-refrangent (or double refracting) when subjected to stress. This double refracting effect depends on the nature and intensity of the applied stresses and disappears on release of the stress. The transmission of light through bi-refrangent flat plates subjected to plane stress within the elastic limits of the material obeys the following laws:

(a) The incident light at any point is resolved into two components which are parallel to the principal stresses at that point.

(b) The velocity of the transmission of each component is dependent on the magnitude of the principal stress in the plane along which it is transmitted.

The difference in velocity of the light ($v_1 - v_2$) in the principal planes is directly related to the difference between the principal stresses ($\sigma_1 - \sigma_2$):

$$\frac{v(v_2 - v_1)}{v_1 v_2} = C(\sigma_1 - \sigma_2) \quad (11)$$

where v = velocity of light in the medium surrounding the photo-elastic model,

v_1 and v_2 = velocity of the light along the principal planes in the photo-elastic model,

C = constant.

The relation between the optical effects and the stress in the model is given by equation:

$$t_1 - t_2 = C/v (\sigma_1 - \sigma_2)T \quad (12)$$

where t_1 and t_2 are the times of emergence of the light rays along the principal planes. The retardation $t_1 - t_2$ between the two waves emerging from the model is directly proportional to the difference in the principal stresses $(\sigma_1 - \sigma_2)$, the thickness of the model T and the photo-elastic constant C/v of the material. By introducing another polarizing element, called the analyser, in the system, the retardation can be made visible as a single wave phenomena through the interference effects of the two waves leaving the analyser. The amplitude of the emerging wave is

$$S = a \sin 2 \alpha \sin \Omega \frac{t_1 - t_2}{2} \quad (13)$$

α being the angle between the plane of vibration of the plane polarized light and the stress σ_1 direction.

Ω = angular frequency of the incident light

a = amplitude max.

Since the intensity of the brightness of the transmitted light is proportional to the square of the amplitude there will be darkening of the image of the model wherever conditions are such that equation (13) is zero. Such dark lines or bands are due to one of two conditions, namely:

(a) Points of constant difference between the principal stresses ($\sigma_1 - \sigma_2$) called "fringes", when

$$\Omega \frac{t_1 - t_2}{2} = 0, \pi, 2\pi \text{ etc.}$$

The bands from (a) also represent lines of equal maximum shearing stress, since

$$\sigma_1 - \sigma_2 = 2\tau_{max}$$

(b) Points of constant stress direction called isoclinics, when $\alpha = 0^\circ$ or 90° .

The previous statements indicate that both fringes and isoclinics appear when models are examined in a plane polariscope. When white light is used there can be no mistaking the isoclinics which appear as black bands on the multi-colored isochromatic background. When

monochromatic light is used, however, both fringes and isoclinics appear as dark lines and to avoid confusion it is desirable to remove the isoclinics for satisfactory examination of the fringes. Circularly polarized light is used for this purpose, and the setup of a circular polariscope is shown in Picture 8. The first quarter wave plate converts the plane polarized light into circularly polarized light by producing a shift in phase of $\pi/2$ between the two waves passing through it, and the second quarter wave plate nullifies this effect. The fringe order can be determined with ease by starting from the zero order fringe. The difference in the principal stresses or the maximum shearing stress are found by equation:

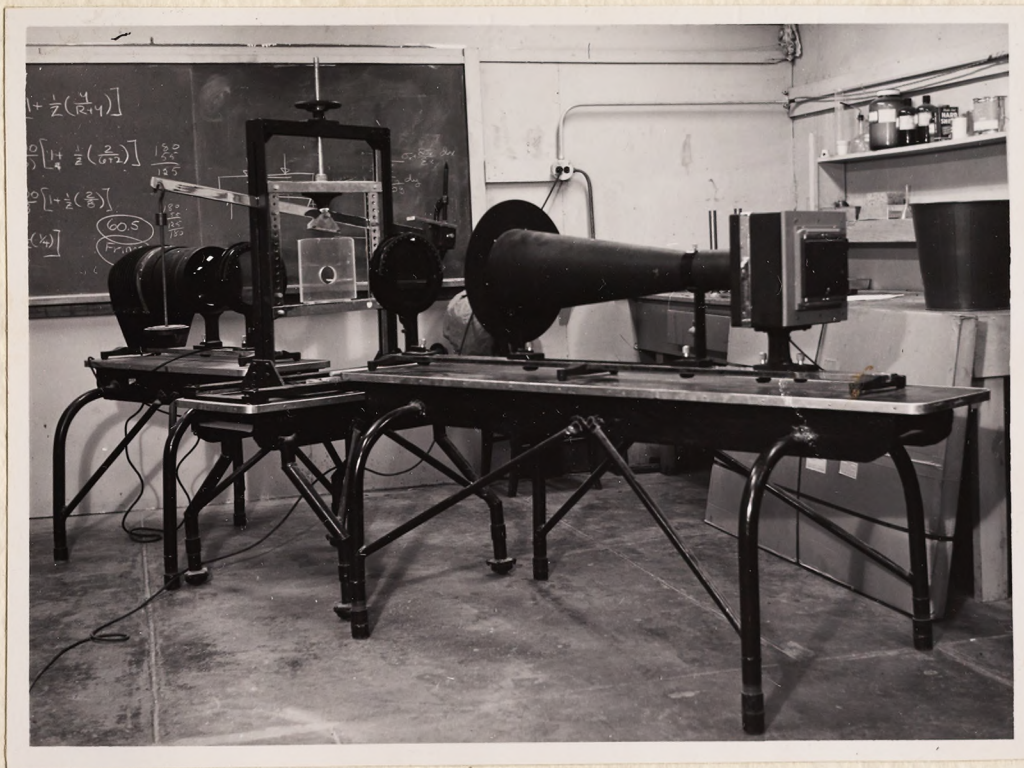
$$\sigma_1 - \sigma_2 = 2 \tau_{\max} = \frac{n f}{T} \quad (14)$$

n = fringe order,

f = material fringe constant,

T = thickness of the model.

The material fringe constant f relating the optical effects and the stresses in a photo-elastic model has a unique value for each birefringent material. Its numerical magnitude can be obtained by calibrating the material by means of a model for which there is a known theoretical solution for the distribution of stresses.



Picture 8. Polariscopes

"Stress-freezing" Technique in Model Study (44, 45, 46, 47)

The utilization of a centrifugal loading device restricts the selection of the model materials. For a photo-elastic analysis, a material demonstrating the phenomena of bi-refringence when under load is required. In addition it should be elastic, transparent and easily machinable. These properties, although present for a number of plastics, were not sufficient for the research contemplated, since a model cannot always be analysed while in a centrifuge, and the photo-elastic characteristics of most plastics normally disappear after removal of the load.

When heated to a specific temperature, some thermo-setting resins become "rubbery" and deform quite easily under small loads (42, 43). If allowed to cool while under load, these resins become rigid again and when the load is removed, it is found that they retain both the strain and the fringe pattern developed while in the thermo-plastic condition. That is, the fringe pattern has been "frozen" into the model; this term being used metaphorically. The investigator is, therefore, free to examine photo-elastically the model at any time after the removal of load.

The stress "freezing" technique was practiced with Alderite B by the National Mechanical Engineering Research Institute of the South African Council for Scientific and Industrial Research, Pre-

toria (HOEK and BERNER⁽⁴⁵⁾ and HOEK⁽⁴⁶⁾). The stresses were frozen in under centrifugal load by means of two insulated furnaces which are attached to each end of the rotor of the centrifuge. Power was delivered to the furnace heaters through heavy current slip rings and the temperature was controlled by means of an automatic temperature controller.

To avoid the problem of heat control in the stress "freezing" technique, a new epoxy resin was developed and tested by the Armour Research Foundation of the Illinois Institute of Technology, (DALLY, DURELLI and RILEY⁽⁴⁴⁾ and DURELLI and KOBAYASHI⁽⁴⁸⁾). Manufactured by the Ciba Company, Inc. Kimberton, Pa., the plastic is known commercially as Araldite 502. The properties of the resin can be varied over a wide range by mixing it with compatible plasticizer such as dibutyl phthalate. The composition used in the study of the above mentioned authors was obtained by mixing 72% resin with 20% dibutyl and 8% araldite hardener HN 951. The manufacture of the plastic was accomplished by mixing the three constituents (all being liquid) in the proper proportions and pouring the resultant mixture into a suitable mold.

Since the chemical reactions between the three constituents with this the curing process, progresses over a time of more than 20 hours, the properties of the material change during this time continuously. The fringe order varies due to a combination of effects:

(a) Creep, which is very pronounced, increases the fringe order at a particular point in the model as a function of time,

(b) The material chemical, mechanical and optical properties change as the curing progresses.

It is important to note, however, that the pattern always represents the elastic distribution of stress in the model while loaded. This fact explains the great advantage of the material.

For a composition of resin/dibutyl/hardener of 72/20/8 proportions, DALLY et al.⁽⁴⁴⁾, determined the change of the properties using a circular disc as an example for three significant times; t_1 , immediately after loading, t_2 , 4 hours after loading (just prior to unloading) and t_3 , 16 hours after unloading (permanently cured).

TABLE 2 (44)

	Poisson's Ratio ν	Modulus of Elasticity E (psi)	Material fringe value f (psi-in/fringe)	Figure of merit E / f (fringe/in.)
t_1	0,366	993	2,44	406
t_2	0,466	675	1,56	432
t_3	0,405	926	2,56	362

In Figure 13 the fringe order is plotted against position on the horizontal diameter of a disc with time as parameter. The curve for t_3 and the corresponding property values can be used in a final analysis.

Application of Model Study to Roof Bolting

As early as 1952, JACOBI⁽²¹⁾ performed the first experiments concerned with the application of roof bolts in stratified rock under symmetrical conditions with gypsum models. He assumed that the foot wall had no influence on the bolting effect and made this part of the model of massive gypsum. Side walls and roof consisted of a sequence of plates of 5 mm thickness each. In models without any bolt support, cracks were observed at the lower surface of the beam in the middle of the span at the point corresponding to the highest bending stress. With increasing load, two other cracks occurred at the top of the beam near the abutments as might be expected. The latter cracks continued downwards and upwards into the next beds, converging to form an arch, showing the well known shape which is often observed underground.

A different behavior was observed for a case where 4 bolts were installed at angles of less than 45° ; two to each side, through 5 beds. Neither arch nor cracks were formed, but instead the whole compound beam was pressed into the abutments. The beam did not

Curve 1 : Immediately after loading
 Curve 2 : 4 hours after loading
 Curve 3 : 16 hours and 64 hours after loading

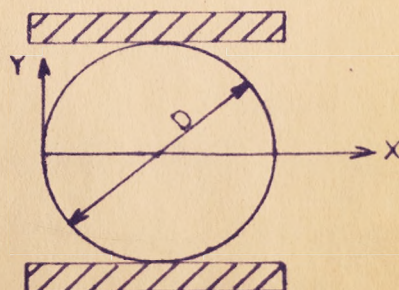
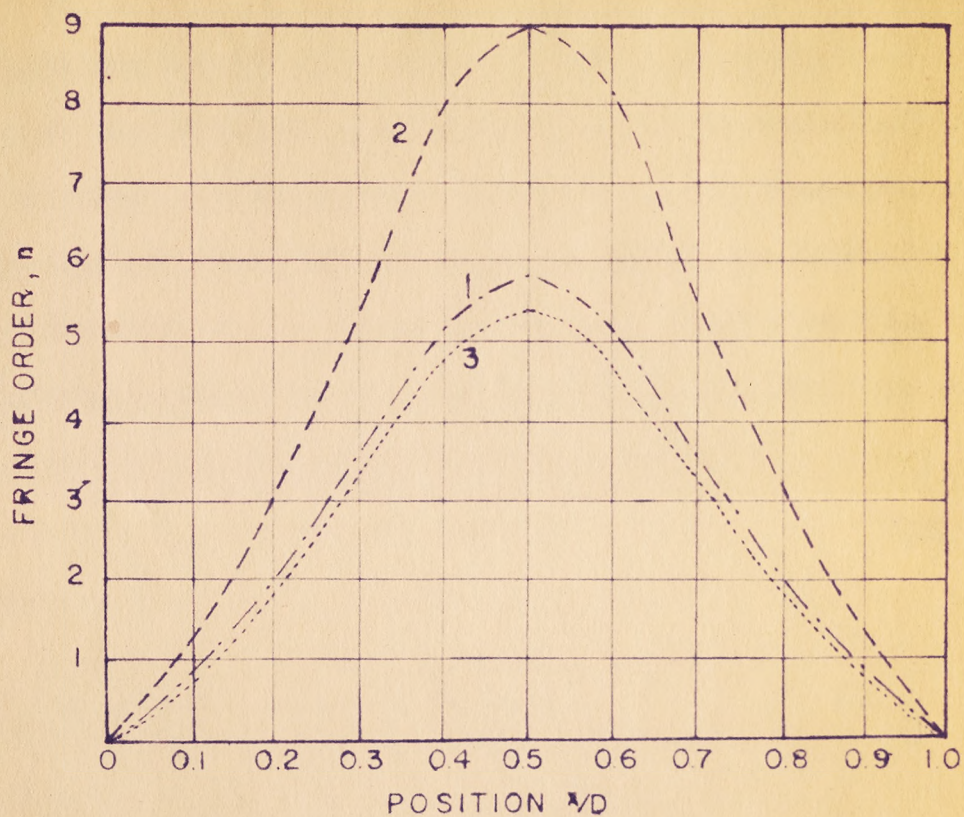


Figure 13

Fringe order along horizontal
 diameter of a disk with time
 as parameter

(after Dally et al.)

fail, when subjected to an even higher load. For this test series, Jacobi used a conventional uniform loading device.

PANEK (32, 34, 35) started a series of symmetrical model tests in 1955, as applied to roof bolts. In order to obtain natural conditions, he used a centrifugal testing apparatus, installed in the Applied Physics Laboratory, Bureau of Mines, U.S. Department of Interior, College Park, Md. His model material was Indiana or Alabama limestone cut to proper dimensions. Panek developed the model-prototype relations by using the dimensional analysis method and obtained two general expressions for roof bolting design formulas for the strain ϵ_x and the deflection D in terms of the structural variables:

$$\epsilon_x = f\left(\frac{AwL}{E}, \frac{P}{EL^2}, \frac{L}{t}, \frac{L}{b}, \frac{h}{t}, K\right) \quad (15)$$

$$D = 0.265 (bL^2)^{-\frac{1}{2}} [KP (h/t - 1)/h] \quad (16)$$

where

P = bolt tension

b = spacing between the bolts

h = length of the bolt

K = bolt per ft., across the opening

Panek assumed that certain model-prototype similarities could be relaxed without invalidating the results and by this, minimized the number of variables to be studied, and extended the applicability of quantitative test data to a large class of full scale structures.

Equation (15) is written for strain rather than for stress, because Panek found it convenient to work directly with strain measurements. Electrical resistance strain gages were bonded to the limestone beds and strains were measured by conventional methods.

The solution of the roof bolting design problem consists of finding a function for the right-hand side of equation (15) which can be used to calculate the effect of the independent variables.

It was mentioned previously in section II B that the reinforcing effect of roof bolts can include a component due to friction and a component due to suspension. While Panek's first series of model studies dealt only with the friction effect, since he used beds with equal thickness, his investigation was later extended to include models built with beds of different thickness⁽³³⁾.

When a sequence of layers is loaded in a centrifuge by variable forces, different flexures will occur for each bed and any model study with roof bolts has to consider both friction and suspension effects. By an iterative trial-and-error method Panek found that the combined effects of friction and suspension are given by:

$$\sigma_{f s} = \sigma_{\eta} (1 + D_f)(1 + D_s) \quad (17)$$

where σ_{fs} = outer-fiber bending stress when both friction and suspension effects are present,
 σ_m = outer-fiber bending stress when neither friction nor suspension effects are present.

The fractional change in the outer-fiber bending stress due to friction, D_f , is given by

$$D_f = 0.375 (bL)^{-\frac{1}{2}} FKP \left(\frac{h/t - 1}{h} \right)^{1/3} \quad (18)$$

and the fractional change in the outer-fiber bending stress due to suspension, D_s , is given by

$$D_s = 1.080 u_1 \frac{K}{K+1}^{\frac{1}{2}} (1 - b/L)^{-1} \left(\frac{h}{t} - 1 \right)^{-1/5} \quad (19)$$

$1 + u_1$ = relative flexural rigidity.

As a final result he derived 3 equations for stress, deflection and coefficient of the bedding-plane friction which are applicable when both friction and suspension effects are present:

$$\sigma_{fs} = (1 + D_f)(1 + \beta D_s) \quad (20)$$

$$\delta_{fs} = (1 + D_f)(1 + \gamma D_s) \quad (21)$$

$$F_{fs} = (\epsilon D_s) Wt b L \quad (22)$$

+ being factors varying with the location and number of points of attachment (bolts). Equation (20) can be used for design purposes, since the reinforcement factor due to bolting may be calculated from it. Equation (21) can be used for field evaluation of a roof bolting system based on roof deflection measurements. Finally equation (22) can be used to calculate the upper limit for the roof bolt tension that is required to prevent strata separation at the bolt location.

In 1956, JOHNSTON⁽³⁶⁾ performed a model study with photo-elastic material and plaster in the laboratory of the Royal Technical College in Glasgow, Scotland. Using a conventional loading device he showed by photo-elastic analysis for a symmetrical opening that roof bolts as a suspension support diminish the bending stress at the lower surface of the beam and the shearing stresses at the abutments. He was able to visualize a similar effect for a compound beam and also for an opening with an arched shape. Calculations in the latter case resulted in a reduction of the bending stresses up to 38% when high pre-tension of the bolts was applied.

The photo-elastic materials used for the construction of the models in this investigation were Columbia resin (CR 39), bakelite (BT/61/893), catalin and perspex, the last being used only for the determination of isoclinic lines. Bolts were made of 0,065 in. diameter wire, threaded to take No. 10 BA nuts with bolt plates and roof bars made from copper sheet.

LANG⁽³⁷⁾ in the United States and KOZINA⁽³⁸⁾ in Russia performed similar photo-elastic studies with plastics of roof bolt situations. In order to find the effect of a single, regular joint pattern in the strata on roof bolt performance, Lang constructed a model of approximately 640 pieces of plastic, 1/4 in. thick. The stress distribution was highly complex and gave no fundamental information.

Finally a model study of BALS⁽⁴⁰⁾ must be mentioned which is of particular interest, since the chosen conditions are closer to the present subject than those of any other investigation. Bals simulated stratified rock in unsymmetrical conditions by paraffine models mixed with sand. He took into consideration that the stresses in the gate-road roof change continuously with the advance of the face (see section II A). Therefore, he assumed that the demonstration of the stress distribution in only one plane across the gate-road was not sufficient and for this reason constructed a three dimensional model as shown in picture 9. The "S"-curve of convergence discussed previously can be followed on one side of the opening and the model shows how the immediate roof is subjected to a continuous change in its bending and shearing stresses. Although Bals did not perform any model studies with roof bolts, he concluded that installation of roof bolts in gate-roads must consider the three dimensional aspect of strata movement. This was deemed possible by inclining the bolts at certain angles to the long axis of the opening as well as to the

abutments. By this means, he believed a solution for roof bolt application at any stage of the passing face was obtained. Two of his pattern proposals, derived from his conclusions, are given in Figure 13.



Picture 9. Three-dimensional Model representing
a Section through a Long Wall Gate-Road (after Bals)

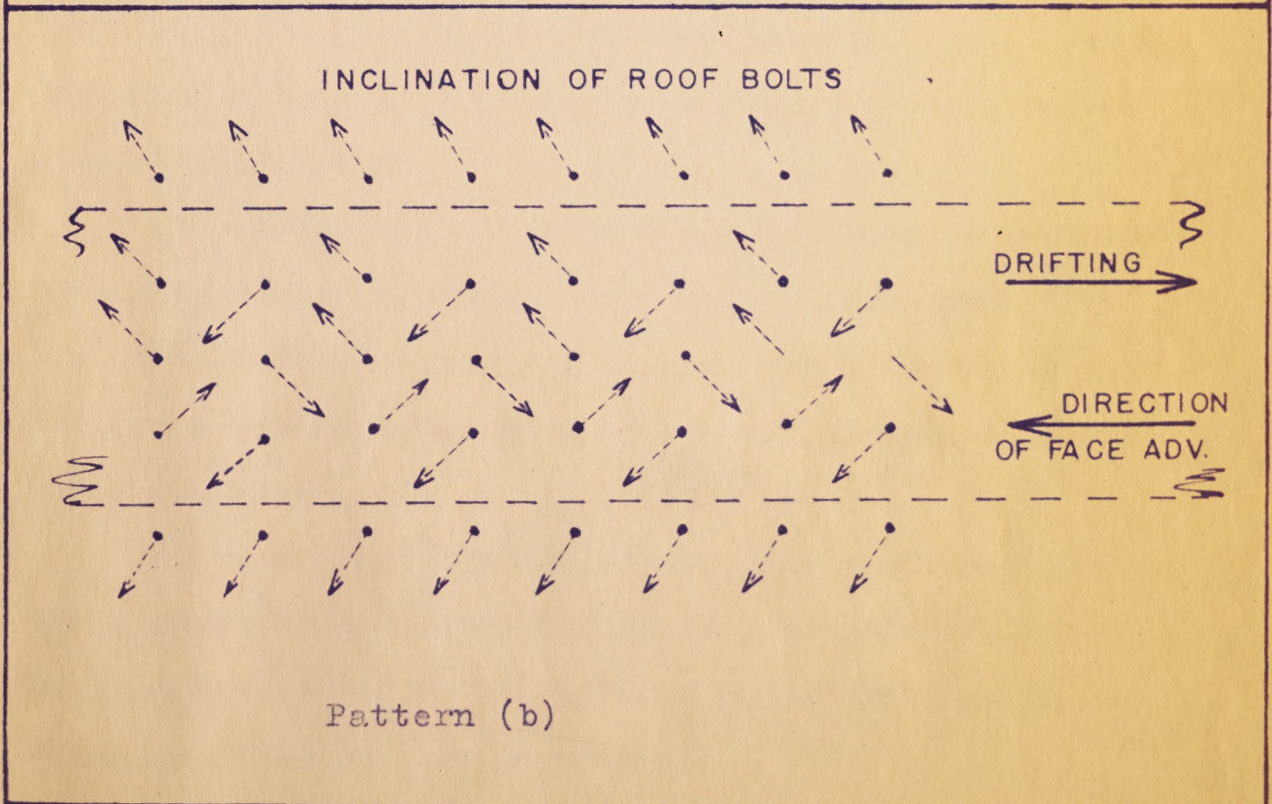
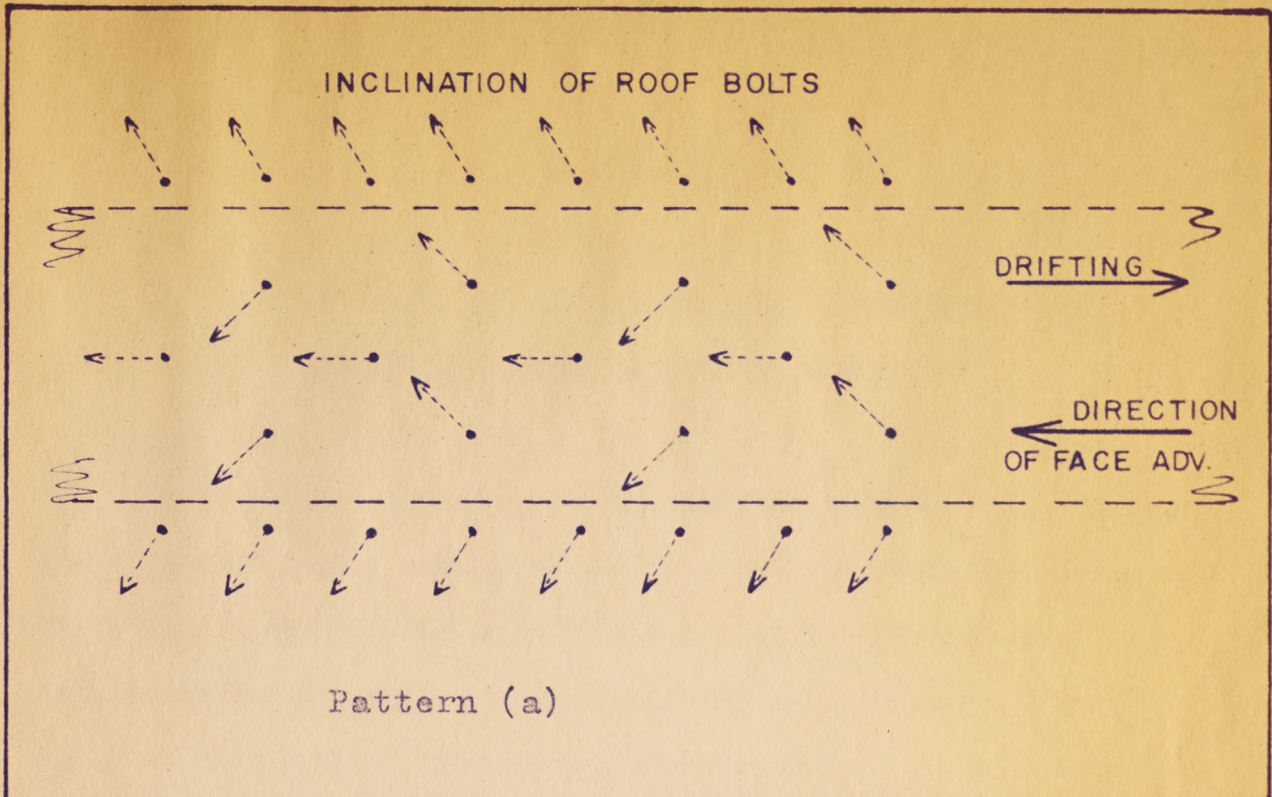


Figure 14

Roof bolt pattern in
long wall gate-roads
(after Bals)

CHAPTER III

MODEL STUDY OF THE APPLICATION OF ROOF BOLTS
UNDER UNSYMMETRICAL LOADING CONDITIONS

Based on the literature study concerned with (1) the stresses and movements in the strata around openings, (2) with the theory and practice of roof bolting in stratified rock and (3) with model study in general and as applied to roof bolting in particular, the following theoretical background, instrumentation and materials were used in the investigation presented in this thesis, to indicate the stress effects of roof bolts in long wall gate-roads by means of small-scale models:

(a) A centrifuge as loading device simulating variable body forces as occur in the strata around long wall gate-roads,

(b) Elastic, transparent and easily machinable models simulating the structural conditions of long wall gate-roads and the surrounding strata,

(c) Epoxy resin Araldite 502 mixed with plasticizer such as dibutyl phthalate and hardener HN 951 as a model material, providing the properties needed for the "stress-freezing" technique in the centrifuge during the test procedure,

(d) Installation of small-scale roof bolts in the models obtaining the anchorage effect by quick-setting cement.

(e) Mechanical cutting, shaping and grinding instrumentation to machine and polish the models after unloading,

(f) Theory of elasticity as applied to optical effects (photo-elasticity) for the theoretical analysis,

(g) A polariscope for the experimental analysis.

Theoretical Background of the Experiments

Referring to discussion of the theory of similitude in the review of literature the stresses in prototypes and that induced in models under load can be expressed by equation (23)⁽⁴⁰⁾.

$$\frac{\tau_{\max_P}}{\tau_{\max_m}} = \frac{w_P L_P}{w_m L_m A} = \frac{E_P}{E_m} \quad (23)$$

where the suffixes p and m refer to prototype and model and

τ_{\max} = the maximum shearing stress at the point under consideration,

w = specific gravity of the material,

A = acceleration applied to the model, in multiples of the gravitational acceleration (g's),

L = span of the opening,

E = modulus of elasticity.

Since a photo-elastic material is used, the maximum shearing stress in the model can be expressed in terms of isochromatic fringes produced under load.

$$\tau_{\max} = \frac{fn}{2T} \quad (24)$$

where f = material fringe value,

n = fringe order at the point under consideration,

T = thickness of the model.

From equations (23) and (24) the fringe order in the model can be related to the maximum shearing stress in the prototype by the following equation:

$$\tau_{\max} = \frac{f n}{2T A} \cdot \frac{w_p L_p}{w_m L_m} \quad (25)$$

The purpose of this experiment is to find the stress distribution in models with and without bolts, and particularly the bending stress at the outer fiber of the immediate roof where failure occurs due to high tensile stresses. On a free unloaded boundary, the principal stresses lie along and normal to the edge, respectively. The principal stress normal to the boundary, determined as σ_2 , is always zero and the equation

$$\tau_{\max} = \frac{\sigma_1 - \sigma_2}{2} \quad (26)$$

reduces to

$$\begin{aligned}\tau_{\max} &= \sigma_1/2 \\ \sigma_1 &= 2\tau_{\max} \\ \therefore \sigma_1 &= \frac{n f}{T} \quad (27)\end{aligned}$$

The fringe order can be determined with the aid of the polariscope and by the use of equation (27) the maximum bending stress for models with and without bolts is found, since the specific material fringe value and the thickness of the model is known. Variation of the bedding plane slip, the "plug-effect", the shearing and tensile reinforcement, although impossible to evaluate separately, influence the stress distribution. The results of a model analysis which includes these factors can give an indication of the bolt pattern with the highest efficiency for the prototype.

Experimental Instrumentation

Centrifugal Testing Apparatus

The centrifugal testing apparatus (Picture 10), installed in the Research Laboratory, Department of Mining Engineering at Missouri School of Mines and Metallurgy, comprises the following basic elements:

- (a) Rotor,
- (b) Model holders and counterweight,
- (c) Housing tank,
- (d) Accessory equipment (balance, vacuum device, motor, speed control and stroboscope).

Rotor. The rotor consists of a boxlike structure made of bare ^{1/2} 1-inch aluminum alloy plate, which is mounted on a vertical 2.5-inch forged steel shaft. The inside dimensions of the rotor are 72 x 33 x 6 inches. This gives a radius of rotation to the base of the modelholder on one, and the counterweight on the other extremity of 36.0 inches. An 18-inch wide opening through the rotor permits observation of the model.

Equation (10) shows that the loading ratio A is proportional to the radius and the square of the speed of rotation. The maximum usable radius of rotation is fixed once the machine is built; during the test series, A was varied by controlling the speed of rotation. To be able to test moderately deep models, it is desirable to have as large a radius as is practicable, thereby minimizing the percentage-wise variation in radius of rotation throughout the depth of the model. The ratio of rotor radius to model depth of 36 : 1.5 inches is insignificant for this study, and, therefore, no corrections for the effect of radius variation across the model depth were considered.

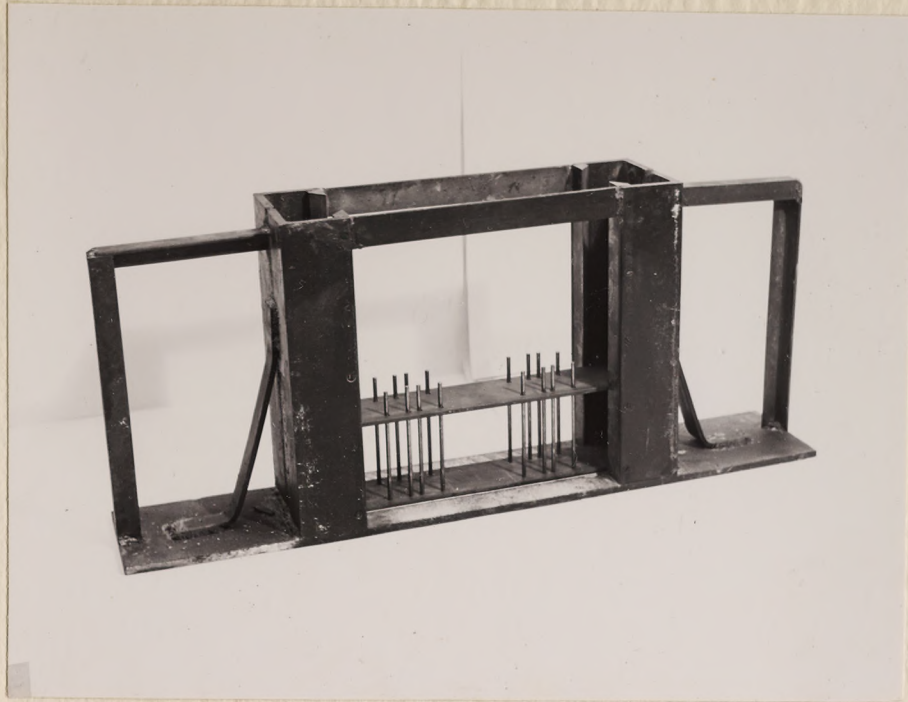


Picture 10. Centrifugal Testing Apparatus.

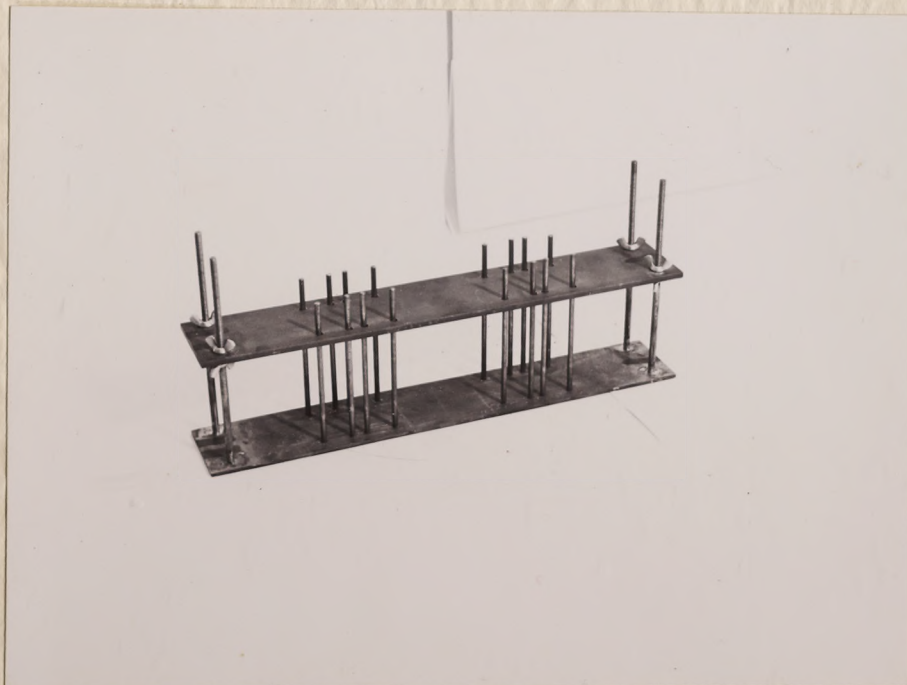
The design of the rotor⁽⁴¹⁾ was based on a maximum speed of 1,500 R.P.M. but for the experiments with plastic as used in this study, the speed always ranged below 500 R.P.M. and did not approach the utmost limit of the capacity.

The upper shaft-bearing housing is bolted to a 15-inch structural steel channel, which is in turn bolted to a supporting framework of 12-inch structural steel channels. The frame system is anchored to concrete walls surrounding the centrifuge tank. The whole installation is mounted on another channel set, 6 feet below the floor level for safety reasons.

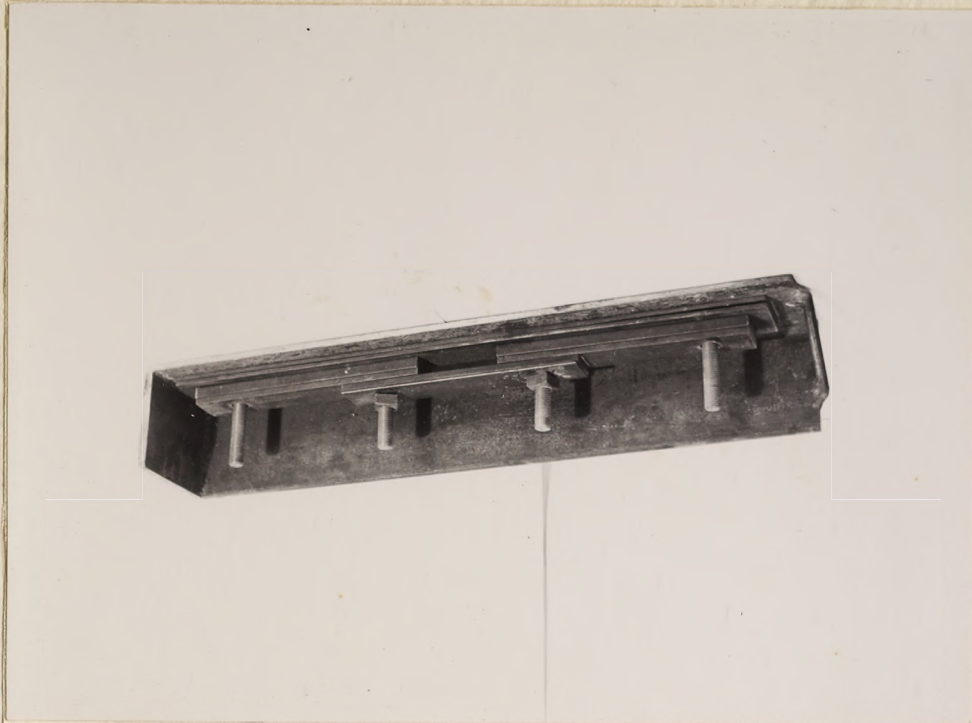
Modelholders and Counterweight. For the study of stratified mine roof, the model consisted of beams lying one upon the other across the opening. Since these composite models were difficult to keep in position during a test, particularly in the unsymmetrical case, a special holding device was constructed. The model was at first mounted in a small model holder (Picture 11) with horizontal dimensions of 17 x 3 inches; the height was varied according to the requirements in different tests by wing nuts. This holder could be set with ease into a larger holding device (Picture 12) and the combination with a total weight up to 90 lbs. was inserted in one wing of the rotor. During the test, the model holder was supported at the end of the rotor, the model beams being vertical (parallel to the axis of rotation).



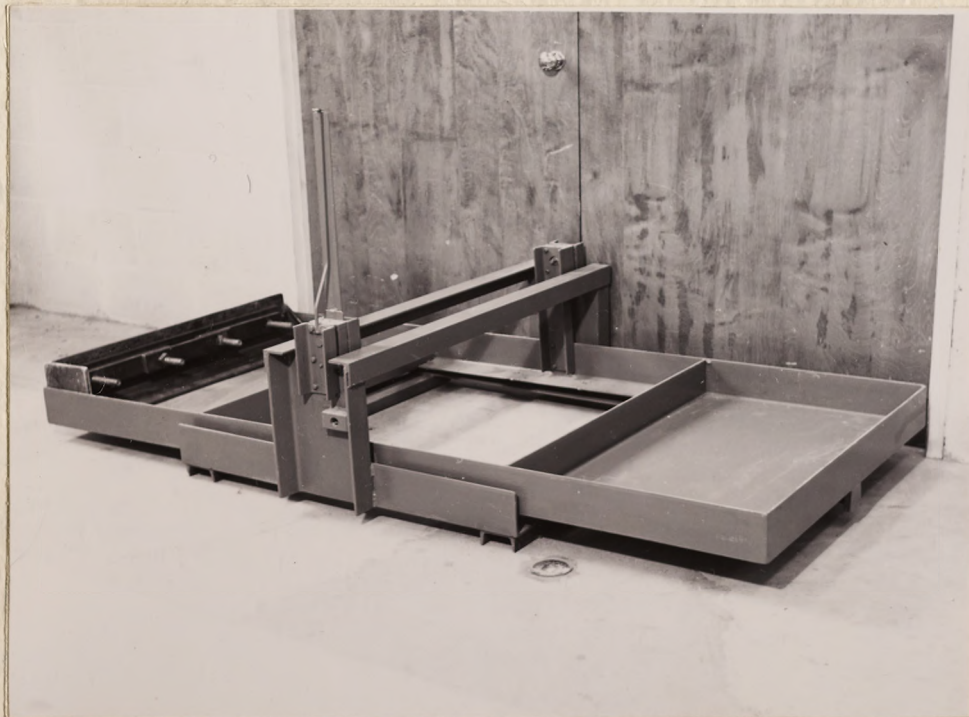
Picture 11. Model Holder I and II



Picture 12. Model Holder II



Picture 13. Counterweight



Picture 14. Balance

The counterweight, similarly supported, consisted of a variable number of interchangeable metal plates of different weight. Its weight was balanced against that of the model holder combination (Picture 13).

Housing Tank. To minimize the driving power required, the centrifuge is operated in a 38-inch diameter tank (Picture 10) in a vacuum up to 28 inches mercury. The tank is welded to the upper and lower shaft-bearing housings and is sealed against the passage of air:

(a) between the flanges joining the head to the lower part of the tank by rubber gaskets,

(b) between the flanges of the two observation ports and the top access port (through which the model holder and the counterweight is inserted) by flat rubber gaskets,

(c) around the shaft where it passes through the head of the tank by a shaft seal.

The two 20-inch observation ports are closed by tempered plate glass portlights one inch in thickness. Two ports are provided, so that either side of the model can be observed and photoelastic measurements can be performed on rotating models, if these are thin and transparent enough.

Accessory Equipment. To avoid vibration and any damage, an exact balance of both wings of the rotor is necessary. Therefore it is not sufficient to check the weight of the model holder and the counterweight by a normal weighing machine, since the center of gravity is in a different position for each item due to the variation in weight distribution. A special apparatus was constructed (Picture 14) duplicating the dimensions of the rotor and proper results could be achieved by adding metal plates to the counterweight until the device showed a balance.

A vacuum of 25-28 inches mercury in the tank was obtained by a vacuum pump, type 30, model V 23 A, manufactured by the Ingersoll-Rand Co. It is a base-mounted, single cylinder compressor driven by an A.C. motor of 3/4 HP.

The driving device for the centrifuge is a motor with specifications: 10 HP, 1,750 R.P.M. base speed, 240 Volt input drawing 38.3 amps at full load. The motor is supplied by a Select A Spede Power Unit (220 Volt, 3 Phase, 60 Cycles) with A.C. input and 230 Volt D.C. output.

A rheostat speed control is combined with the driving set of the centrifuge, which enables the operator to maintain acceleration, deceleration and constant speed with ease.

A strobe light mounted in each observation port and directed towards the opposite port, flashes on the rotor when it is at the

correct position for viewing. A slip ring around the shaft contacts strobe trigger brushes which provide a steady illumination of either the specimen or the counterweight for five different positions of the rotor (0° , $\pm 5^{\circ}$ and $\pm 10^{\circ}$). The view provided by the strobe lights in the centrifuge is brought to the level of the operating console by means of a periscope.

Photo-elastic Equipment

A photograph of the polariscope used, installed in the Laboratory for Experimental Stress Analysis, Mechanics Department, M.S.M., is reproduced in Picture 9. This instrument is a lens type bench polariscope which has a 12 inch-diameter parallel light field. It can be used for transmitted light, photo-elastic studies. The optical components have been corrected for the use with monochromatic green light (5,461 Angstrom units) produced by a high-pressure mercury vapour lamp. The polarizer, analyser and quarter wave plates can be rotated by hand as required in the analysis. A camera was used in conjunction with the polariscope to obtain direct photographs of the fringe distributions in the "stress-frozen" models.

Model Design

Since the "stress-freezing" technique described in Chapter II was used in this study, Araldite 502 was chosen as model material and was mixed with dibutyl phthalate plasticizer and hardener HN 951. Preliminary tests for developing an experimental technique for the use with unsymmetrically loaded models led to the conclusion that convenient dimensions for the construction of the model were:

beam depth	= 0.5 in.
beam length	= 9.0 in.
model thickness	= 1.5 in.
span of the opening	= 3.0 in.
height of the opening	= 1.5 in.

These measurements were limited partially by the construction of the centrifuge and the model holder, respectively, and partially by the acceleration effects of the centrifuge. A model less than 1.0 in. thickness was found to be affected by even slow angular accelerations, when it was not confined on both sides, and bending in the third dimension and twisting occurred, when one abutment was replaced by sheets of foam rubber in order to simulate the unsymmetrical case. To eliminate this distortion a thickness of 1.5 in. was chosen. The height of the opening was unimportant because it did not affect

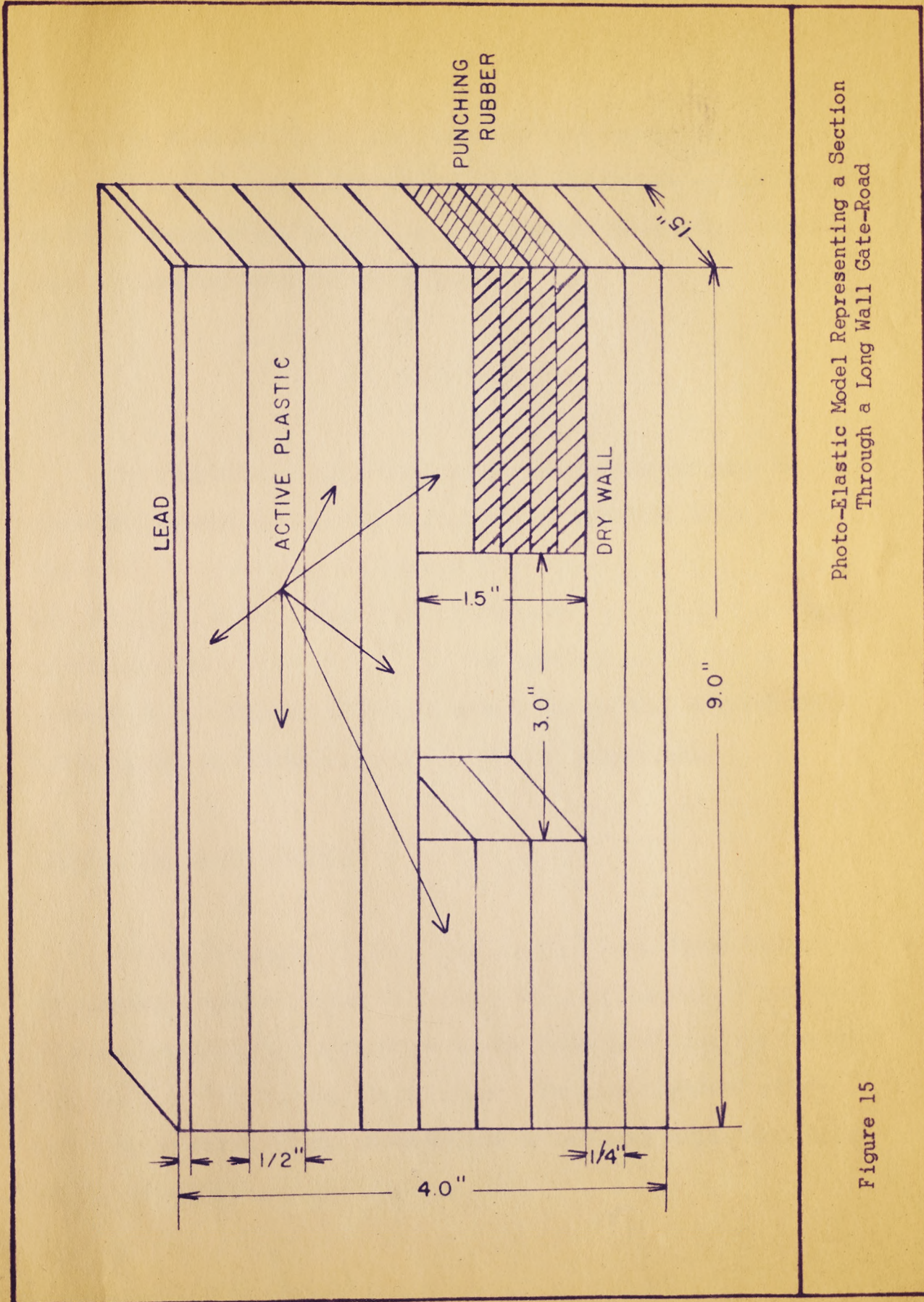


Photo-Elastic Model Representing a Section Through a Long Wall Gate-Road

Figure 15

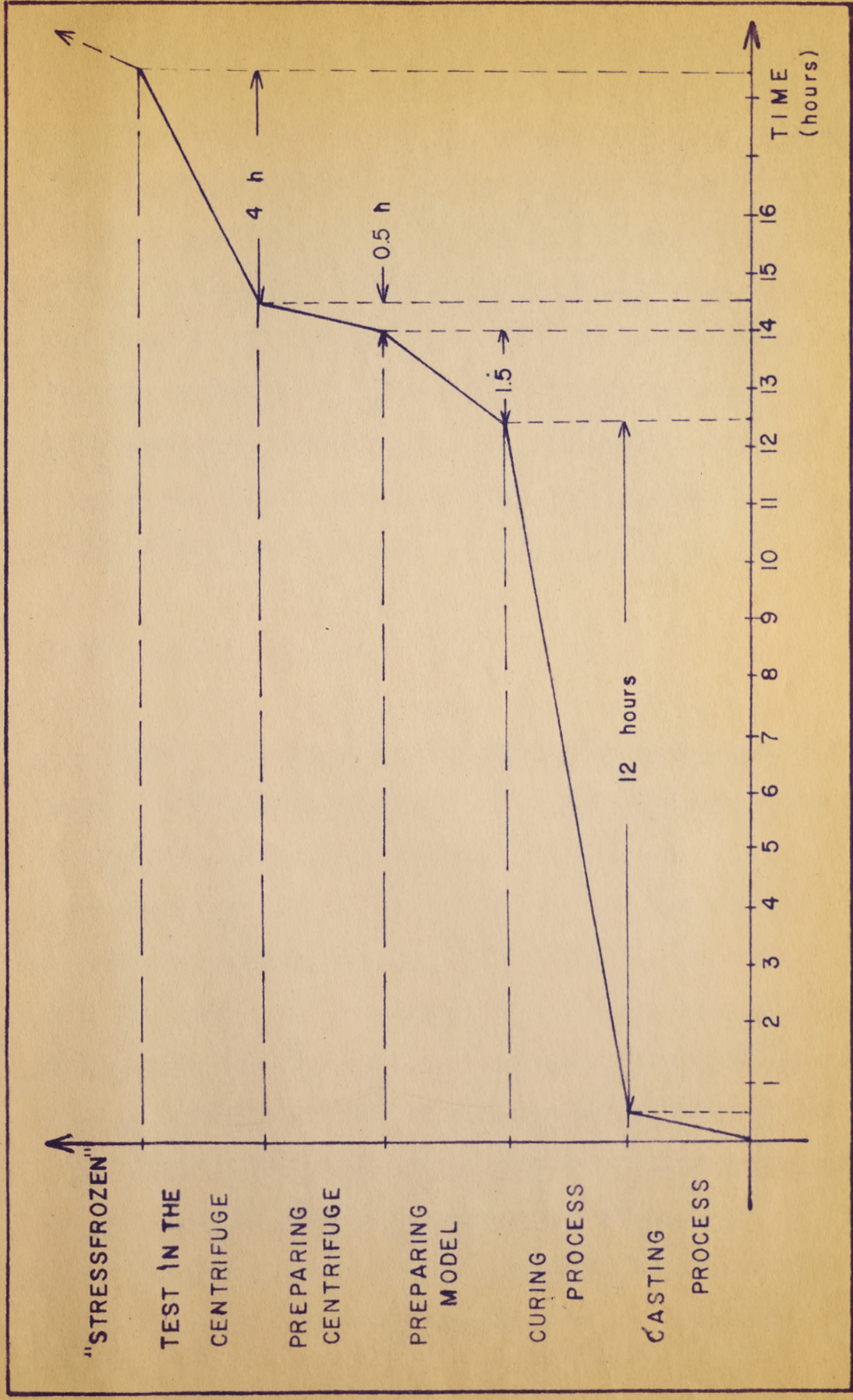
the stress distribution in the immediate roof around the bolts. Figure 15 shows a three-dimensional model incorporating the features outlined above, which was cut into convenient slices for analysis when the loading process was finished.

Test Procedure

The significant properties of the photo-elastic material as described previously and the various time dependent steps during the test procedure made a standard time schedule necessary. This was developed after a series of preliminary tests following the experiences of DALLY et al. ⁽¹⁴⁾. The schedule was followed as closely as possible to eliminate errors due to time effects in the material and to obtain comparable results (Figure 15).

Casting and Curing Process

To build a model as described above, it was found convenient to prepare a mold as shown in Picture 15. Two plates of lucite were clamped together with spacers on three sides providing the required thickness of 0.5 in. for the plastic. The low viscosity of the epoxy resin mixture made it necessary to securely tape three sides of the mold to avoid any possible leak.



Standard Time Schedule for the Test Series Including the "Stress-Freezing" Process

Figure 16

The three constituents were weighed carefully to obtain a 72/20/8-ratio of epoxy resin, dibutyl phthalate and HN 951 hardener and mixed in a beaker of suitable size. After stirring approximately 5 min. the mixture was poured into the mold and its exterior was kept under a steady temperature of 78° F. By this means some of the heat developed by the exothermic reaction between the hardener and the resin was carried away. No mold release material was needed since it was easy to remove the semi-cured plastic from the lucite plates after about 12 hours.

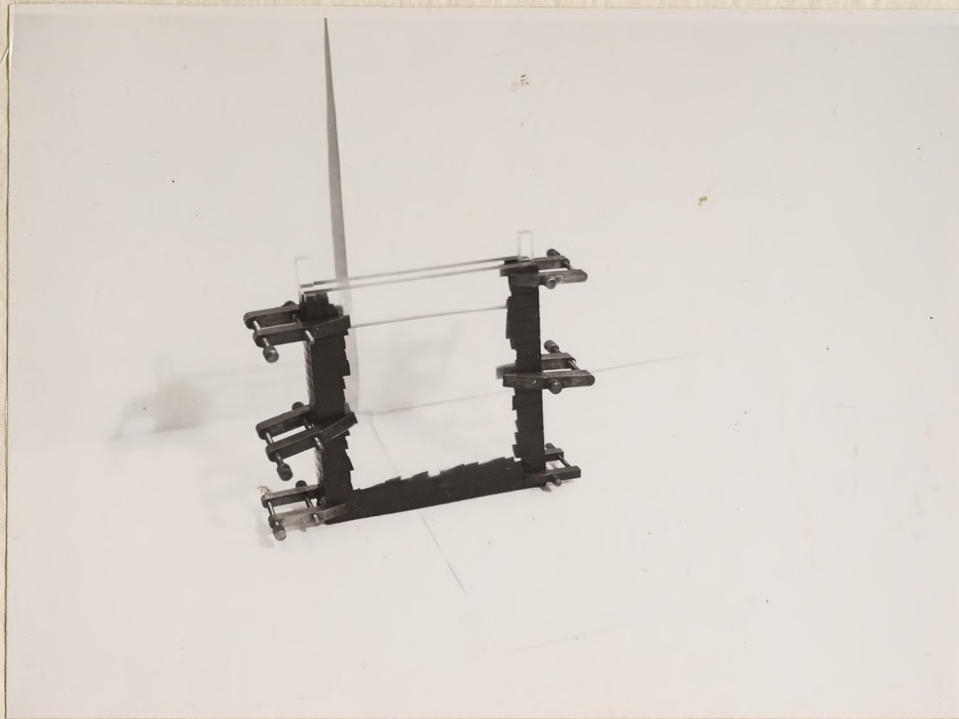
Preparing Model for Test

After 12 hours, a plastic with the consistency of a hard rubber eraser was obtained. The plate, 12 x 6.5 x 0.5 in. in dimensions, was cut with a band saw, forming 4 beams of 9.0 x 1.5 x 0.5 and 2 beams of 3.0 x 1.5 x 0.5 in. The beams were put together to fabricate a model representing the area affected by one roof bolt set across a long wall gate-road. No changes were made in the construction of the model during the final test series. Both sides of the composite model were planed by means of a shaper and a uniform thickness of 1.50 in. was maintained. It was verified that the machining process did not cause any residual stress in the plastic.

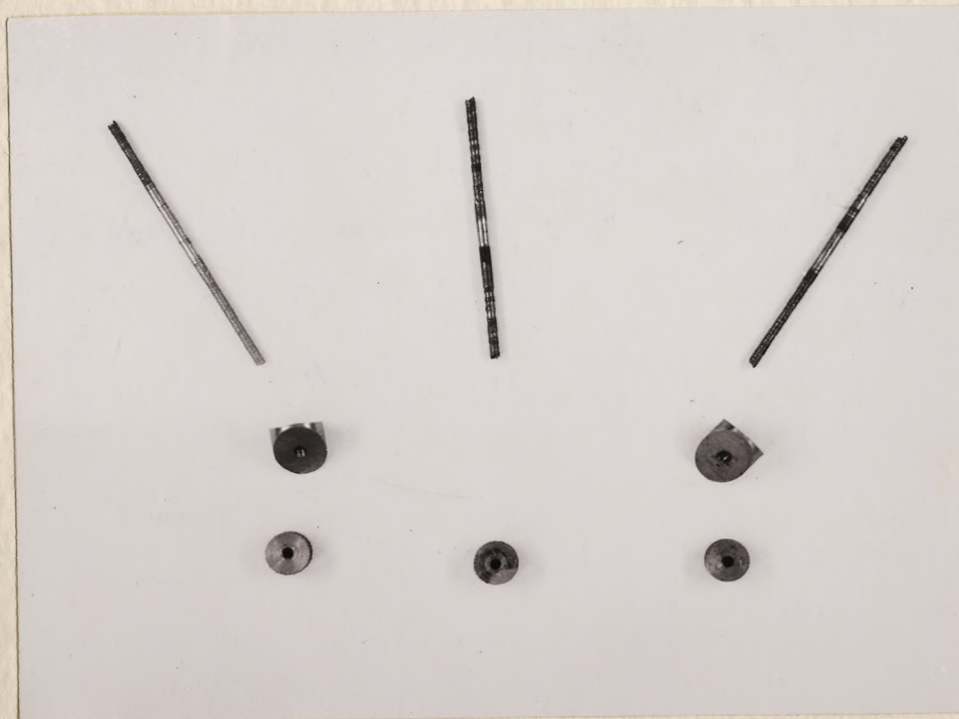
Since only the roof and one layer in the abutment strata were constructed from active plastic the model was completed with beams

of reinforced gypsum sheets. For the unsymmetrical case, two of the plastic beams in the abutment were replaced on one side by four foam rubber sheets (Picture 15). The model was completed with a lead sheet of $1/16$ in. in thickness on top increasing the effective weight of the model under centrifugal load.

Roof bolts were installed in this model study, using for the first time a new method developed successfully in the German Coal Mining Industry for full scale structures, in which the anchorage effect is obtained by a quick setting cement. In the full scale application, cartridges filled with resin and a separate container with hardener are pushed into the hole with the bolt and destroyed so that the resin-hardener mixture glue the threaded bolts to the rock⁽²³⁾. A seal around the bolts keeps the resin in position until after a setting time of 30 min. pretension can be applied. Although the technique of installation was simplified in the model study, the basic idea of this kind of anchorage effect was utilized. Steel bolts of $1/16$ in. in diameter and proper length were threaded on both ends. One end was emersed in cement (Eastman 910 Adhesive) and inserted into the $3/32$ diameter holes. After a setting time of approximately 20 min., the bolts were prestressed with steel nuts by hand. Washers constructed for various angles provided proper installation of the bolts (Picture 16).



Picture 15. Mold for the Casting Process



Picture 16. Roof Bolts, Washers and Nuts as used in the Model study.

Loading Process

The rotation of the centrifuge about a vertical axis made it necessary to mount the model in such a way that the beams would be vertical. Model holder II (Picture 12) was designed to provide this position of the model during the test. The upper steel plate of this device was adjusted before each test so that it barely touched the model. When load was applied, the model separated from the plate and was only influenced by its own weight, since the plate was kept in position by stopnuts and its $3/16$ in. thickness resulted in a negligible bending. This separation was actually observed by means of the stroboscope and was estimated to be up to 0.5 in. on the yielding side. Eight steel bolts on each side of the model holder prevented shifting of the model. This device was found necessary since several tests had to be stopped because the model changed its position or even fell free in the tank. After balancing the model holder combination (I and II) against the counterweight, both items were inserted through the access port into the rotor wings and the model was placed in the center of the observation opening of the rotor. The vacuum was brought up to about 15 in. mercury before the centrifuge was started; the required speed being reached after approximately 15 min. running and kept constant with high accuracy over the whole length of the loading process of 4 hours. Although

a considerable amount of material creep occurred during the test, the results are not invalidated as was mentioned previously in the discussion of the "stress-freezing" technique.

Preparing the Model for Analysis

After a running time of the centrifuge of 4 hours, the curing process was finished for the purpose of the test and the stress distribution which had existed under load was "locked" in the model. At this point, however, an analysis of the fringe pattern developed in the centrifuge was not possible, since the thickness of 1.5 in. showed a high interference and absorbed too much light of the polariscope. The model thickness had to be reduced and, since the fringe distribution observed in the model is dependent on the thickness (equation (27)), an accurate method was required. An attempt was made to keep the temperature during the machining process as low as possible, since it was not known, what effect heat could have on a stress-frozen model. While cooling the exterior with an electric fan, a shaper was used, set on low speed and taking light cuts to decrease frictional heat. During the first part of the test series the models were shaped to a thickness of $1/2$ in. Later this was reduced to $3/8$ in. to obtain more distinct fringe patterns which were found to be very complex.

In a further improvement of the specimen preparation for analysis, the surfaces of the slices were polished on both sides on a grinding table. Aluminum oxide was used as a polishing material and as a result, "stress-frozen" models representing an approximate two-dimensional section through a long wall gate-road where roof bolts are installed was obtained (Picture 17 and 18). The fringe patterns could be read with relative ease and photographs were taken as permanent records.

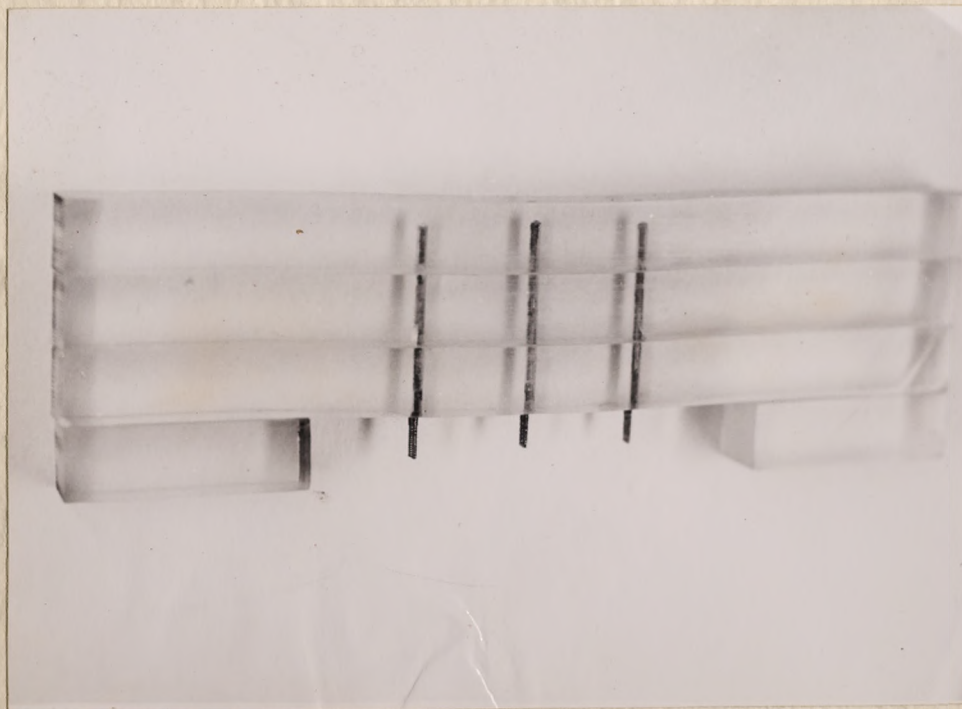
Analysis of the Models

The experimental investigation included 20 tests in the centrifuge designed to give information about the "stress-freezing" technique, in general, and roof bolt installations in stratified rock, in particular. The test data and the correlating remarks are listed in Table III, and photographs of some of the fringe patterns are shown in Pictures 19 - 29.

The test series was started with models representing a symmetrical case, to prove that the body loads developed in the centrifuge act symmetrical within the model. Since there is negligible difference in the bending and shearing stresses in a symmetrical beam, whether it is loaded by uniform load, its own weight or centrifugal forces, the stress distribution and the fringe pattern, as it should



Picture 17. Unsymmetrical Model after Shaping and Polishing.



Picture 18. Symmetrical Model after Shaping and Polishing with Roof Bolts.

TABLE III

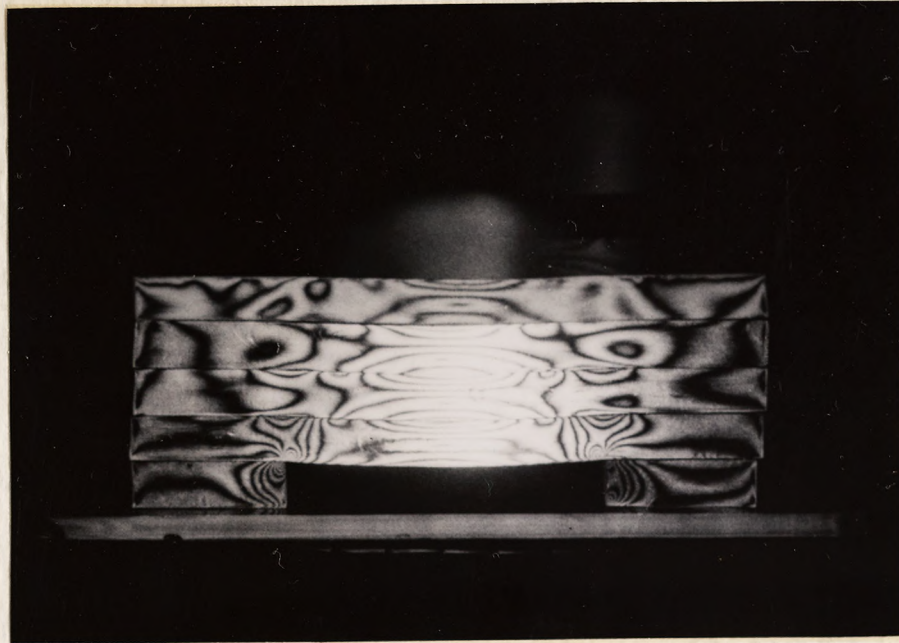
Date of Test	No. of Test	Symmetry of Loading	Roof Bolt Support H.= Holes; B.= Bolts	R.P.M.	A "g's"	Remarks
April 27, 62	1	Sym.	None	350	117	Poor isochromatics
April 29, 62	2	Sym.	3 H. (90°, 90°, 90°)*	350	117	Symmetrical Fringe Pattern, Hole-Displacement not equal on Both Sides.
May 3, 62	3	Unsym.	3 H. (90°, 90°, 90°)	350	117	Model broke after 2 Hours.
May 8, 62	4	Unsym.	3 H. (90°, 90°, 90°)	300	86	Model changed Position in the Model Holder.
May 10, 62	5 ⁺	Unsym.	3 H. (90°, 90°, 90°)	400	152	Holes do not influence Stress Distribution, Proper Hole Displacement.
May 15, 62	6	Sym.	None	360	123	Symmetrical Fringe Pattern
May 16, 62	7	Unsym.	None	360	123	Reading of Fringe Order Possible.
May 23, 62	8	Sym.	3 B. (90°, 90°, 90°)	360	123	Anchorage Effect not Equal for all 3 Bolts

* Indication of the Bolt or Hole Inclination across the Opening; the Direction of Inclination is shown by Arrows.

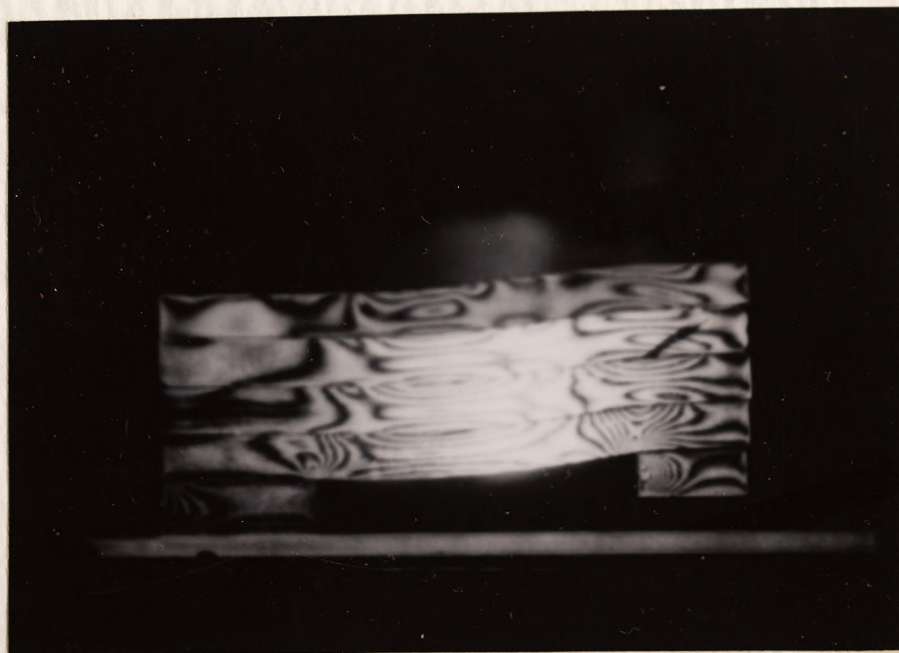
+ Change in the Construction of the Model Holder.

TABLE III (Continued)

Date of Test	No. of Test	Symmetry of Loading	Roof Bolt Support H.= Holes; B.= Bolts	R.P.M.	A "g's"	Remarks
June 23, 62	9	Unsym.	3 B. (90°, 90°, 90°)	360	123	Lower Beam failed in Tension near the center Bolt
June 24, 62	10	Unsym.	3 H. (45°, 90°, 45°)	360	123	Failure in Tension in the Lower Beam
June 25, 62	11	Unsym.	3 B. (45°, 90°, 45°)	360	123	Fracture Zones around the Bolts
June 27, 62	12	Unsym.	1 B. (- , 90°, -)	300	86	Three Beams of the Immediate Roof showed Tension Cracks around the Bolts.
June 29, 62	13	Unsym.	None	300	86	Change in Yielding Device, Proper Fringe Pattern.
June 30, 62	14	Unsym.	3 H. (90°, 60°, 45°)	300	86	No Influence of the Hole, to the Stress Distribution.
July 1, 62	15	Unsym.	3 B. (90°, 60°, 45°)	300	86	No exact Determination is Possible.
July 2, 62	16	Unsym.	1 B. (- , - , 45°)	250	86	Good Results
July 5, 62	17	Unsym.	2 B. (- , 45°, 45°)	300	86	Good Results
July 6, 62	18	Unsym.	1 B. (60°, - , -)	300	86	Good Results
July 8, 62	19	Unsym.	3 B. (90°, 90°, 90°)	300	86	Good Results
July 9, 62	20	Unsym.	3 B. (60°, 60°, 45°)	300	86	Good Results



Picture 19. Test (6): Fringe Pattern of a Symmetrical Model.



Picture 20. Test (7): Fringe Pattern of an Unsymmetrical Model.

appear, was known from tests with conventional loading devices. In tests (1) and (2), symmetry was not obtained. An indication of the horizontal strata movement was, however, visible in test (2) as displacements in the three vertical holes drilled through the beams. The hole at the opening midspan showed no displacement. Although the isochromatics were found to be unsymmetrical, probably due to uncontrolled eccentricities in the model or model holder design, the test showed that the bolt holes before bolt installation did not influence the fringe pattern. Test (6), performed as a repetition of test (1), at a later date, incorporated model holder changes developed in the intervening series of tests. As shown in Picture (19), the bending stresses are similar in each of the three beams immediately above the opening while the stress concentration above both abutments decreases rapidly from the lower to the upper beam.

In test (3), where the first unsymmetrical model was loaded, the specimen fell free in the tank. As a consequence, the number of "g's" was reduced from 117 to 86 (300 R.P.M.) in test (4), but once again, parts of the model changed position in the model holder, when the convergence on one side was increased by the acceleration process, and the experiment had to be stopped. After the change in the construction of the model holder II described previously, another unsymmetrical model was tested (5) at a speed of 400 R.P.M. (152 "g's"). The first useful results were obtained from this experiment, since

the hole displacements gave an indication of the strata movement under unsymmetrical conditions and the most distinct fringe pattern, up to that time, allowed qualitative readings, although not sufficient for precise analysis.

A test of an unsymmetrical model loaded without any holes or bolts was performed in experiment (7). Picture (20) of the fringe pattern in the model gave the first measurements of the change in stress distribution which occurred when the rigidity of one abutment was reduced, as simulated in the unsymmetrical model. From the corner of the rigid abutment, high stresses propagated upwards into the upper beams with particularly high bending stresses in the top fibers of the first and second beam. In comparison with the symmetrical case (Picture (19)), the shearing stresses have increased and decreased, over the rigid and yielding abutment, respectively. In the symmetrical case, the bending curve shows two symmetrically located points of inflection, which coincided with zones of maximum shear, as can be observed in Picture (19). In Picture (20) illustrating the unsymmetrical conditions, the zone of shear near the rigid abutment is (a) more distinct and (b) has moved towards the middle of the opening, while the shear magnitude near the yielding abutment has diminished. A later repetition of test (7), test (13), performed under lower loading conditions, confirmed the first results and showed an even more pronounced differ-



Picture 21. Test (13): Fringe Pattern of an Unsymmetrical Model.



Picture 22. Test (8): Fringe Pattern of an Unsymmetrical Model with three Vertical Roof Bolts.

ence in the shear stress in comparison with the symmetrical case, as seen in Picture (21).

The location of the point of inflection nearest the rigid abutment will depend on the amount of convergence in the yielding abutment and on the rigidity of the strata comprising the beams. In this investigation a complete analysis of the variation in location of this point was not attempted, since the convergence and the beam stiffness was kept constant; however, there is no doubt that the exact location of this shear zone near the rigid abutment must be considered in the application of roof bolts. The influence of the inflection points on the roof bolt pattern will be discussed in detail in the analysis of the later experiments.

Experiments with actual roof bolt applications were continued based on the information obtained about the unsymmetrical stress distribution in a bedded strata above openings. However, before bolt patterns were tested for unsymmetrical cases, a simple symmetrical model was chosen to evaluate the anchorage method utilized in this study. No previous knowledge existed as to the influence of a bolt which is cemented to the surrounding material over its whole length, on the stress distribution in the strata. Conventional roof bolts are anchored only at one extremity, and have contact with the surrounding rock only if shear forces are applied to them by bed displacements. With cement as a continuous, rigid filler between

the bolt and the hole wall, a bolt can take and transfer stresses at any point over its length. By this phenomena, stress concentrations in small areas, i.e. around the wedge or shell, and the washer of a conventional bolt, can be prevented and can be distributed to all beams in which the bolt is cemented. In test (8) the first attempt was made to glue three vertical bolts, equally spaced over the opening span, through three beams. Although the resultant fringe pattern shows some asymmetry, which may partially be due to unequal pre-tension of the bolts, it can be stated qualitatively that the bending stresses which occur are considerably decreased and the shear zone near the right abutment in Picture (22) is less distinct. Stress concentrations near both corners of the opening above the abutment were reduced. It is worth mentioning that the reduction was equal on both sides of the opening although the two outer bolts had different effects on the material in their immediate area. In the case of the bolt on the left side, in Picture (22), where complete bonding probably occurred only in the upper beam and which is therefore comparable with conventional bolt installation, the only major effect was a reduction of the stress concentration over the abutment. The difference in stress distribution around these two bolts might have been partly due to higher pretension of the left hand bolt.



Picture 23. Test (14): Fringe Pattern of an Unsymmetrical Model with three Holes (45° , 60° and 90°).



Picture 24. Test (15): Fringe Pattern of an Unsymmetrical Model with three Roof Bolts (90° , 60° and 45°).

In spite of the success of test (8), the following tests gave no further information. In test (9), three bolts were installed in the same pattern as in test (8), in an unsymmetrical model, but tension failure was observed in the lower beam near the center bolt. The results of test (10) are shown in Picture (30), where three holes were drilled as cited in Table III. The lower beam failed in tension over the rigid abutment followed by a tension crack at the other end after full load was applied for two hours (360 R.P.M.). Test (11) and (12) again developed fractures when roof bolts were installed under unsymmetrical loading conditions, indicating the high magnitude of the stress developed under certain unsymmetrical loading conditions.

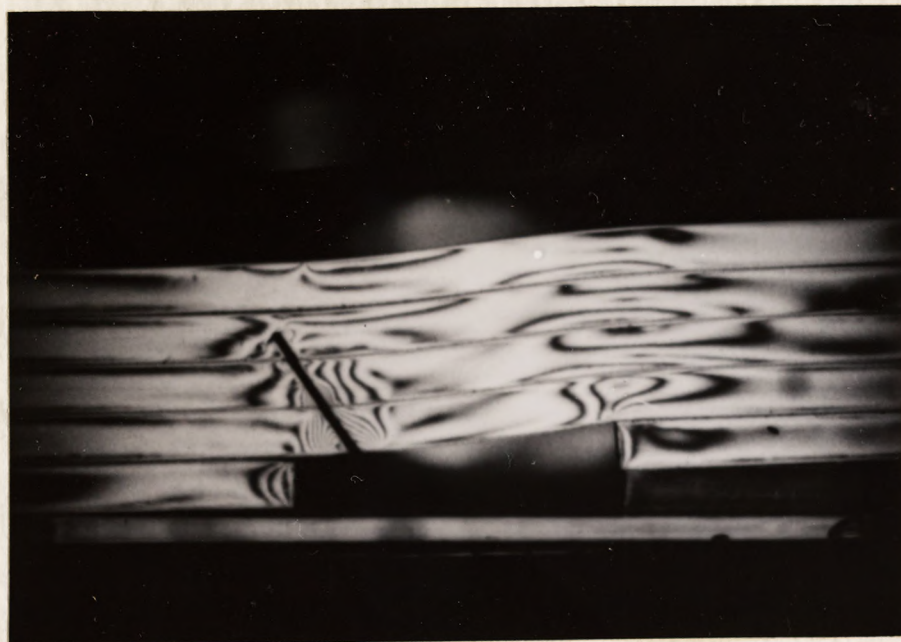
The rigidity of the yielding abutment was reduced during the later tests so that the deflection curve of the beams in the roof of the opening contained only one inflection point, corresponding to the curve most commonly seen in the roof strata during long wall mining operations. This change produced higher bending stresses in the beams, and, therefore, the test series was continued with a lower applied load (86 "g's" at 300 R.P.M.). Test (13) was a duplication of test (7) under these new conditions and the presence of a single point of inflection was verified. In the next seven tests (14 - 20), all structural and nearly all loading conditions were kept constant, and only the hole and bolt pattern was changed to systematically



Picture 25. Test (16): Fringe Pattern of an Unsymmetrical Model with one Roof Bolt (45°).



Picture 26. Test (17): Fringe Pattern of an Unsymmetrical Model with two Roof Bolts (45° and 45°).



Picture 27. Test (18): Fringe Pattern of an Unsymmetrical Model with one Roof Bolt (60°).



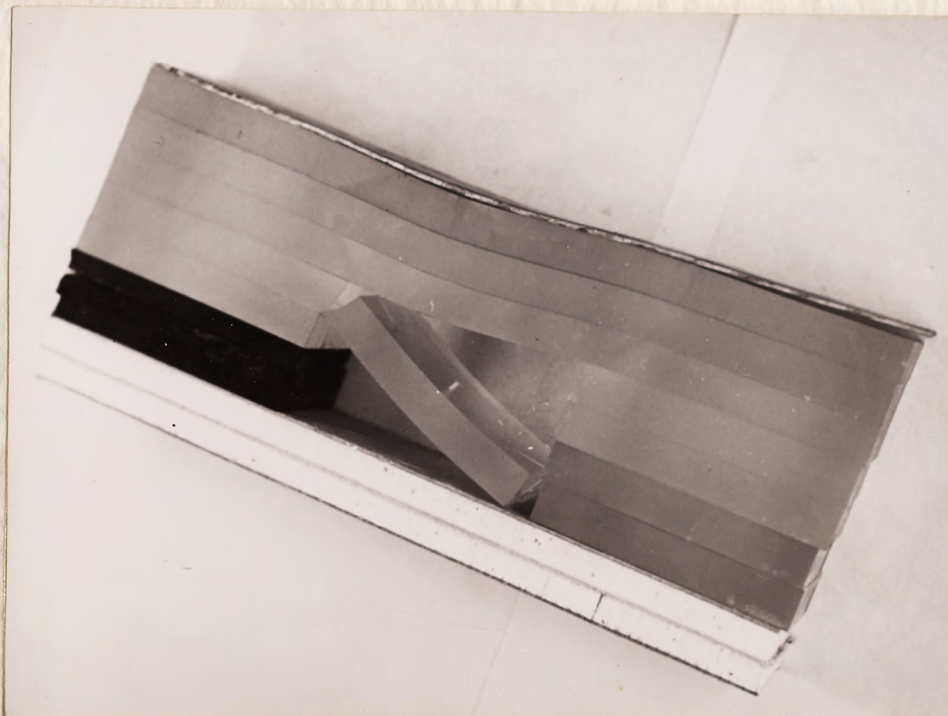
Picture 28. Test (19): Fringe Pattern of an Unsymmetrical Model with three vertical Roof Bolts.

find the best roof bolt pattern. Three holes at different angles (45° , 60° and 90°) from left to right in picture (23), indicate the relative amounts of displacement at these points in test (14). In test (15), three bolts were installed with inclinations of 90° , 60° and 45° , respectively. The purpose of the vertical bolt was to decrease the bending stresses in the left portion of the roof beam in picture (24); the center bolt was to reduce the zone of shear at the point of inflection by utilizing tensile forces developed in the bolt as a restraint; and the bolt to the right was installed to transfer stress from the immediate roof beam above the opening further into the abutment. Qualitatively, this pattern seemed to be successful, but it appeared desirable to investigate the effect of individual, cemented bolts on the stress distribution.

Tests (16) and (17) were performed to determine the effect of roof bolts installed in the vicinity of the rigid abutment on the stress distribution in the strata overlying the opening (Pictures 25 and 26). Bolts inclined away from the opening (45°) reduced the bending stresses in the strata over the rigid abutment. Only a negligible change was observed in the bending stress near the yielding abutment. It must be mentioned that complete bolt to plastic bonding was not achieved in test (17), where two bolts at an angle of 45° were installed in the maximum shear zone and adjacent to the rigid abutment. A proper installation of roof bolts at the small



Picture 29. Test (20): Fringe Pattern of an Unsymmetrical Model with three Roof Bolts (45° , 60° and 60°).



Picture 30. Test (10): Unsymmetrical Model with three Holes (45° , 90° and 45°). The lower Beam failed in Tension near both Abutments.

scale used in this study was found to be extremely difficult.

A single bolt was used in test (18) and set at an angle of 60° adjacent to the yielding abutment. The inclination was chosen to transfer some of the bending stress which occur in this portion of the roof beam to less highly loaded surroundings. The fringe pattern of this test in picture (27) indicates that although a lower load was applied in this case than in previous tests, the stress distribution at the yielding abutment was improved by the presence of a single roof bolt, as was predicted.

In test (19), the adverse effect roof bolts can create if they are installed without consideration of the stress distribution was vividly presented; picture (28). Although the three vertical bolts build a compound beam reducing the high bending stresses over the opening and the shear stresses at the points of inflection which were noticed previously in models without bolts, the bending stresses above the rigid abutment are greatly increased and indicate possible points of tension failure in the series of three beams.

Finally, in test (20), a bolt pattern was developed applying the experiences gained from previous tests and correcting the common mistakes illustrated in test (19). The overall lower stress concentrations resulting with this bolt pattern, picture (29), prove that the complicated unsymmetrical stress distribution can be controlled in models by the proper application of roof bolts. Although the

experiments were performed within the elastic limits of the material, which is not true of the underground prototype, the qualitative results are applicable to full scale structures such as long wall gate-roads, where rock strata may be considered pseudo-elastic. Since the installation of cemented roof bolts affected the readability of the isochromatics developed in the models, a quantitative analysis was inconclusive and possible only within narrow limits which do not permit formulation of quantitative expressions for roof-bolt - rock strata behavior.

CHAPTER IV

SUMMARY AND CONCLUSIONS

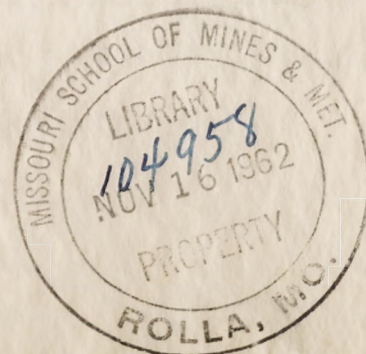
Summary

The purpose of the research presented in this thesis was to investigate the effect of roof bolts on the stability of the strata in the surroundings of long wall gate-roads. When coal is extracted on one side of these openings, convergence occurs and unsymmetrical loading conditions result. In practice, it is extremely difficult to control the strata behavior by conventional methods of support and attempts have been made to strengthen the beds by installation of roof bolts.

In the review of literature the following items were discussed: (a) pressure and relaxation movements in the surroundings of long wall gate-roads, (b) theory and practice of roof bolting in stratified rock and (c) model study in general, and as applied to roof bolting in particular. This discussion introduced the reader to the present investigation. Photo-elastic material as Araldite 502 epoxy mixed with dibutyl phthalate plasticizer and HN 951 hardener was used to fabricate composite models which simulated the strata conditions in the surroundings of long wall gate-roads. Support

for the roof beams consisted of a rigid abutment of plastic, and an abutment made up of foam rubber sheets to obtain a yielding effect and to develop an unsymmetrical configuration. The models were tested in a 6 ft. diameter centrifuge providing the body force load required to satisfy the "principles of similitude". The particular properties of the photo-elastic material utilized enabled the author to "freeze" the stress distribution in which existed during the test in the model. After relieving the load, the original thickness of the model of 1.5 in. was reduced in a machining process and the surfaces were polished to obtain model slices of $3/8$ to $1/2$ in. thickness for analysis in a polariscope.

The test series was started with models under symmetrical conditions to develop the "stress-freezing" technique in the centrifuge and to establish the validity of the results, since the stress distribution for symmetrical cases was known. When subsequent models with a yielding abutment were tested, the stress distribution was found to be different. A zone of high shearing stress was observed in the immediate roof beams near the rigid abutment where the bending inflection point was located. The portion of the lower beam between the shear zone near the rigid abutment and the yielding abutment showed bending stresses similar to those in a symmetrically loaded beam.



Based on this information, roof bolts were installed in the models using a cement to obtain an anchorage effect over the full length of the bolts. Number, inclination and pattern arrangements of the bolts were varied over a series of 13 tests and the results were compared.

Conclusions

The model study presented substantiates the feasibility of application of the "stress-freezing" technique with photo-elastic materials, such as epoxy resin to centrifuge tests with composite models. Therefore, this technique could be applied to a practical mining problem, such as the investigation of the installation of roof bolts in mine openings which show asymmetry in the surrounding strata. Gate-roads accompanying an advancing long wall face are typical of these conditions.

From the results of the model tests simulating long wall gate-roads placed in simple geological structures, it was concluded that the unsymmetrical conditions caused by the extraction process of coal on one side result in a stress distribution with the following significant features:

- (1) The bending stresses above the rigid abutment are greater, and more pronounced in the overlying beams than in the symmetrical case, indicating points of possible tension failure.

(2) The two inflection points in the strata which occur above an opening under symmetrical conditions are reduced to a single point in the unsymmetrical case if the convergence of the yielding abutment is large enough. This single inflection point is located in the beams over the opening in the vicinity of the rigid abutment. Since the inflection point coincides with the zone of high shear, visual observation of the inflection in the strata bending permits determination of the shear zone location across the opening.

(3) The portion of the lower strata between the inflection point and the yielding abutment acts like a beam under symmetrical conditions.

(4) The shear stresses near the yielding abutment are reduced considerably in comparison to those present in a symmetrical condition, where pertinent dimensions are equal.

From analysis of the stress distribution developed in an unsymmetrical model configuration combined with the knowledge of the mechanical behavior of bolts, a bolt pattern with highest efficiency for strengthening the roof strata can be derived. Within the limitations of the assumptions made, of equal modulus of elasticity and thickness of each layer, flat formation and absence of bonding between the layers, the following consideration for the installation of roof bolts can be recommended:

(1) Long bolts should be installed near the rigid abutment extending upward from the critical area above the opening, angling towards the abutment to decrease the high bending stresses.

(2) Bolts should be installed diagonally through the shear plane at the point of inflection of the bending strata utilizing tensile forces developed in the bolt as a restraint.

(3) Bolts should be installed at angles of 60° to 90° , near the yielding abutment, to transfer the bending stresses in that portion of the lower beam between the point of inflection and the yielding abutment to less highly loaded surroundings in the overlying beams.

An extension of the present experimental investigation to more complicated conditions, such as different thickness in the sequence of layers, different modulus of elasticity and considerations of an inclined strata is recommended to obtain further information about the application of the roof bolts in underground openings.

REFERENCES

1. Mueller, L. (1956) "Felssicherungen und verankerte Stützmauern", Z. Der Bau und die Bauindustrie, Fachblatt f. Bautechn. u. Bauwirtschaft, Dusseldorf, H. 10.
2. Busch, A. (1919) "Strecken Ausbau mit eisernen Ankern", Zeitschrift für d. Berg- Hutten- und Salinenwesen 67, p. 7.
3. Baldwin, (1956) "Was this the Beginning of Roof Bolting?" Mechanisation, Aug. p. 61.
4. - (1960) "National Reports" International Conference on Strata Control, Paris, May 1960.
5. Panek, L. A. (1951) "Stresses about Mine Openings in a Homogeneous Rock Body", Edwards Brothers, Inc. Ann Arbor, Michigan.
6. Obert, L., Duvall, W. I. and Merrill, R. H. (1960) "Design of Underground Openings in Competent Rock", Bulletin 587, Bureau of Mines.
7. Dorstewitz, G. (1940) "Spannungsoptische Untersuchungen als Beitrag zur Klärung von Gebirgsspannungen um bergmannische Hohlräume", Archiv f. bergbaul. Forschung, H. 1.
8. Sonntag, G. (1960) "Spannungsoptische und theoretische Untersuchungen der Beanspruchung geschichteter Gebirgskörper in der Umgebung einer Strecke", Forschungsberichte des Landes Nordrheinwestfalen, No. 861.
9. Sonntag, G. (1960) "Die Beanspruchung des Hangenden in Abbaubetrieben mit Vollversatz auf Steinkohlengruben", Gluckauf No. 96 H. 7, p. 434.
10. Creuels, F. H. and I. M. Hermes (1956) "Messung von Gebirgsdruckänderungen in der Nahe der Abbaufrent" Internationale Tagung u. Gebirgsdruckforschung, Druck: Steinkohlenbergbauverein.

11. Jacobi, O. (1960) "Der Druck auf Floz und Versatz" Gluckauf No. 96, H. 7, p. 409.
12. Staasen, P. and R. Liegeois, (1960) "Differing Behaviour of a Type of Rock in a Gate-road as affected by the Method of Driving and Supporting", International Conference on Strata Control, Paris.
13. Schwartz, B. (1960) "Prediction of Rock Movement in Roadways", International Conference on Strata Control, Paris.
14. Schwartz, B. (1960) "Untersuchungen der Gebirgsbewegungen um bergmannische Hohlräume" Bergbauwissenschaften Jahrg. 7, No.9/10.
15. Dubois, R. (1960) "The Various Factors governing Face Convergence" International Conference on Strata Control, Paris.
16. Atkinson, F. S. (1960) "Back Abutment Pressures", Min. and Quarry Engng. 26 No. 3, p. 114/117.
17. Hilbig, R. (1957) "On the general Validity of Lehmann's Trough Theory" Proceedings of the European Congress on Ground Movement, Leeds.
18. Flake, R. (1959) "Untersuchungen über den Zusammenhang zwischen dem Gang der Kohle und der Konvergenz des Nebengesteins", Gluckauf No. 95, H. 14, p. 857.
19. Hoffmann, H. (1956) "Entspannungsbewegungen des Flozes und seines Nebengesteins in der Nahe des Strebstobes", Internationale Tagung über Gebirgsdruckforschung, Essen, Druck: Steinkohlenbergbauverein.
20. Graebisch, W. (1956) "Messungen und Deutung der Bewegungsvorgänge im Gesteinsmantel einer Abbaustrecke vor dem Strebstob", Internationale Tagung über Gebirgsdruckforschung, Essen, Druck: Steinkohlenbergbauverein.
21. Middendorf, H. und Jacobi, O. (1952) "Ankerabau in Abbaustrecken" Gluckauf No. 88, H. 25/26, p. 636.

22. Hoevens, W. and H. Rolshoven (1952) "Betriebsversuche mit Ankerausbau auf dem Steinkohlenbergwerk Consolidation unter Berücksichtigung amerikanischer Erfahrungen", Gluckauf 88, H. 11/12, p. 281.
23. Krippner, E. (1958) "Ankerausbau in Abbau- und Gesteinsstrecken", Gluckauf No. 94, H. 7/8, p. 267.
24. Schuermann, F. (1960) "Measures against the Relaxation Movements occurring in Roadway Walls" International Conference on Strata Control, Paris.
25. Fritzsche, C. H. (1956) "Bergbaukunde" Springer Verlag Göttingen Heidelberg, Berlin, Germany.
26. Lewis, R. S. (1955) "Elements of Mining" John Wiley and Sons, Inc., New York.
27. Schuermann, F. (1959) "Die Anwendbarkeit des Ankerausbaus im Westdeutschen Steinkohlenbergbau", Diss. T. H. Aachen.
28. Thomas, E. (1954) "Rock Bolting finds wide Application" Mining Engineering, Nov. p. 1080.
29. Schmuck, H. K. (1956) "Theory and Practice of Rock Bolting" The Colorado School of Mines Quarterly, Volume 52, No. 3, p. 235.
30. Bucky, P. B. (1950) "Theory of Roof Bolting" Coal Mine Modernization, Yearbook.
31. Jacobi, O. (1952) "Zur Statik des Ankerausbaus" Bergfreiheit 17, No. 1, p. 9.
32. Panek, L. A. (1956) "Principles of Reinforcing Bedded Mine Roof with Bolts" Bureau of Mines, Report of Investigations No. 5156.
33. Panek, L. A. (1961) "Use of Vertical Roof Bolts to Reinforce an Arbitrary Sequence of Beds" International Symposium on Mining Research
34. Panek, L. A. (1956) "Theory of Model Testing as applied to Roof Bolting", Bureau of Mines, Report of Investigation, No. 5154

35. Panek, L. A. (1956) "Design of Bolting Systems to Reinforce Bedded Mine Roof", Bureau of Mines, Report of Investigations No. 5155.
36. Johnston, A. G. (1956) "Roof Bolting in Mines, Theory and Practice", Iron and Coal Trades Review 173, p. 1077.
37. Lang, T. A. (1961) "Theory and Practice of Rock Bolting" Trans. AIME, Feb.
38. Kozina, A. M. (1959) "Untersuchungen des Verhaltens beim Ankerausbau an Modellen aus gleichwertigen Stoffen", Ugol 34, No. 4, p. 25/29.
39. Guminskij, M. V. (1960) "Untersuchungen von Fragen des Gebirgsdrucks noch der optischen Polarisationsmethode im Zentrifugalfeld", Izvest. Akad. Nauk. SSSR. Met. Topl. No. 3.
40. Bals, R. (1956) "Eignung des Gebirgsankerausbaus zur Erleichterung des Streckenvortriebs im Steinkohlenbergbau" Forschungsberichte des Landes Nordrhein-Westfalen No. 269.
41. Panek, L. A. (1952) "Centrifugal Testing Apparatus for Mine-Structure Stress Analysis", Bureau of Mines Report of Investigations 4883.
42. Caudle, R. D. and Clark, G. B. (1955) "Stresses around Mine Openings in some simple geological Structures" University of Illinois, Engineering Experiment Station Bulletin No. 430, Vol. 52, No. 69.
43. Haber, D. F. (1962) "A Study of the Stress Distribution around Circular Openings using Multilayered Photo-elastic Material", Thesis Missouri School of Mines and Metallurgy.
44. Dally, J. W., Durelli, A. J. and W. F. Riley (1957) "A New Method to "Lock in" Elastic Effects for Experimental Stress Analysis", ASME Applied Mechanics Division Paper No. 57-A-71.
45. Hoek, E. and G. Berner (1961) "The Use of Photo-elasticity for Experimental Stress Analysis", South African Council for Scientific and Industrial Research, Pretoria.

46. Hoek, E. (1961) "The Application of Experimental Mechanics to the Study of Rock Stress Problems encountered in Deep Level Mining in South Africa", Reprint of a Paper presented to the International Congress on Experimental Mechanics, New York.
47. Bucky, P. B. and A. L. Fentress (1934) "Application of Principles of Similitude to Design Mine Workings", A.I.M.E., T.P. 529, 1934.
48. Durelli, A. J. and A. S. Kobayashi (1957) "Stress Distributions around Hydrostatically loaded circular Holes in the Neighborhood of Corners", ASME Applied Mechanics Division Paper No. 57-A-4.
49. Frocht, M. M. (1957) "Photo-elasticity", Vol. 1, John Wiley and Sons, Inc., New York.
50. Chan, S. M. (1960) "Physical Property Tests of Rock, Centrifugal Tests and the Design of Underground Mine Openings" Thesis, Missouri School of Mines and Metallurgy.

VITA

Friedrich Hermann Karl E S S E R, son of Dr. Friedrich Esser and Agnes Boytinck, was born on April 12, 1932 in Rheinberg, Germany. Since 1938 the author attended several elementary schools and high schools and he received the Maturity in Moers, Germany, in 1952.

After a practical training of one year in various kinds of underground operations (coal, salt and metal mines) he was enrolled in the Bergakademie Clausthal for the study of Mining Engineering. During 1955 and 1956 he continued his studies for two semesters at the Technical Universities in Berlin and Stockholm, Sweden, before he returned to Clausthal, where he received the degree "Diplomingenieur" (M.S.) in November 1957.

Subsequently, the author started a special training of 4 years arranged by the Department of Mining of the German government as a further education both for Civil Service and management. In June 1961 he finished the requirements and examinations for the degree and title "Assessor des Bergfachs".

In September 1961 the author was appointed for 9 months as a Graduate Assistant in the Department of Mining Engineering at the University of Missouri, Missouri School of Mines and Metallurgy, and was the recipient of a Fulbright Travel Grant given by the United States Government.

At Missouri School of Mines and Metallurgy the author studied towards the degree "Master of Science in Mining Engineering" and became a member of the Honorary Earth Science Fraternity Sigma Gamma Epsilon.